

NASA TECHNICAL NOTE



NASA TN D-3127

NASA TN D-3127

c 1

LOAN COPY: RETURN
AFWL (WLIL-2)
KIRTLAND AFB, NM

0130149

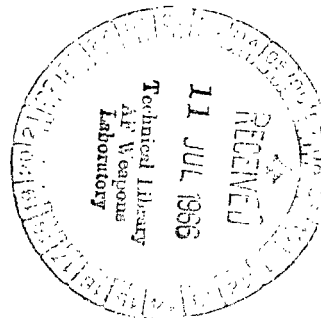


TIROS VII INFRARED RADIATION COVERAGE OF THE 1963 ATLANTIC HURRICANE SEASON WITH SUPPORTING TELEVISION AND CONVENTIONAL METEOROLOGICAL DATA

by Lewis J. Allison and Harold P. Thompson

Goddard Space Flight Center

Greenbelt, Md.





TIROS VII INFRARED RADIATION COVERAGE
OF THE
1963 ATLANTIC HURRICANE SEASON
WITH
SUPPORTING TELEVISION AND CONVENTIONAL
METEOROLOGICAL DATA

By Lewis J. Allison and Harold P. Thompson

Goddard Space Flight Center
Greenbelt, Md.

NATIONAL AERONAUTICS AND SPACE ADMINISTRATION

For sale by the Clearinghouse for Federal Scientific and Technical Information
Springfield, Virginia 22151 - Price \$2.00

ABSTRACT

Eight tropical cyclones of the 1963 North Atlantic hurricane season were studied using Tiros VII Channel 2 (8-12 μ) radiation data. Seventeen computer-produced radiation charts were analyzed in order to delineate the three dimensional cloud structure over these storms. Time cross-sections were drawn over Hurricanes Cindy and Edith in order to relate the warm core development and upper-level outflow of the storms with their respective cloud canopies, as shown by the radiation data.

Tiros VI and VII television pictures and nephanalyses, aerial reconnaissance weather reports, radar photographs, radiosonde data, and conventional synoptic analyses were used to complement the Tiros VII radiation data.

An attempt was made to correlate minimum equivalent blackbody temperatures T_{BB} measured by the satellite over the tropical cyclones with maximum observed surface wind speeds. However, the minimum T_{BB} values were found to vary from 205 to 220°K in several stages of hurricane development, and no significant relationship between tropical cyclone intensity and cloud top heights could be found from the limited data sample available.

CONTENTS

Abstract	ii
INTRODUCTION	1
METHOD OF ANALYSIS	1
THE 1963 NORTH ATLANTIC HURRICANE SEASON	5
Hurricane Arlene	5
Hurricane Beulah	8
Hurricane Cindy	13
Hurricane Debra	19
Hurricane Edith	23
Hurricane Flora	29
Hurricane Ginny	32
Tropical Storm Helena	40
SATELLITE RADIATION DATA AND HURRICANE RESEARCH	44
CONCLUSION	46
ACKNOWLEDGMENTS	46
References	47

TIROS VII INFRARED RADIATION COVERAGE OF THE 1963 ATLANTIC HURRICANE SEASON WITH SUPPORTING TELEVISION AND CONVENTIONAL METEOROLOGICAL DATA

by

Lewis J. Allison and Harold P. Thompson
Goddard Space Flight Center

INTRODUCTION

One of the most significant achievements of the Tiros medium resolution radiometer experiments has been the demonstrated capability of the radiation data to detect and track storm systems in data-sparse areas of the world, at night as well as in the daytime (References, 1, 2, 3). This report is an attempt to demonstrate that the Tiros VII radiation data also can provide valuable three-dimensional views of tropical cyclones in various stages of development which besides leading to certain conclusions in this paper, should prove to be useful for hurricane research in the future.

Synoptic weather charts, Tiros VI and VII television pictures and nephanalyses, radiosonde data, radar data and aircraft weather reports were used to complement the Tiros VII radiation analysis.

METHOD OF ANALYSIS

The synoptic weather and position reports for each of the eight tropical cyclones which occurred during the period 31 July to 30 October 1963 were obtained from the U.S. Navy Hurricane Hunter flights (Reference 4) and the U.S. Weather Bureau charts and official reports (References 5, 6, 7, 8, 9). A history of the storm tracks of the 1963 hurricane season is shown in Figure 1 (Reference 7).

The index of Tiros VII Final Meteorological Radiation Tapes was carefully screened during the life history of each storm and the relevant subpoint orbital tracks were drawn for a preliminary cross-check of possible storm coverage (References 10 and 11).

Tiros VII radiation grid print maps (1:10 million scale) for the 8 to 12 μ atmospheric window region were printed out for all orbits which could contain possible storm data (Table 1). Seventeen orbits were selected for their optimum storm coverage and were rerun on a 1:5 million scale. This scale was chosen because it averaged one to ten individual measurements which provided for

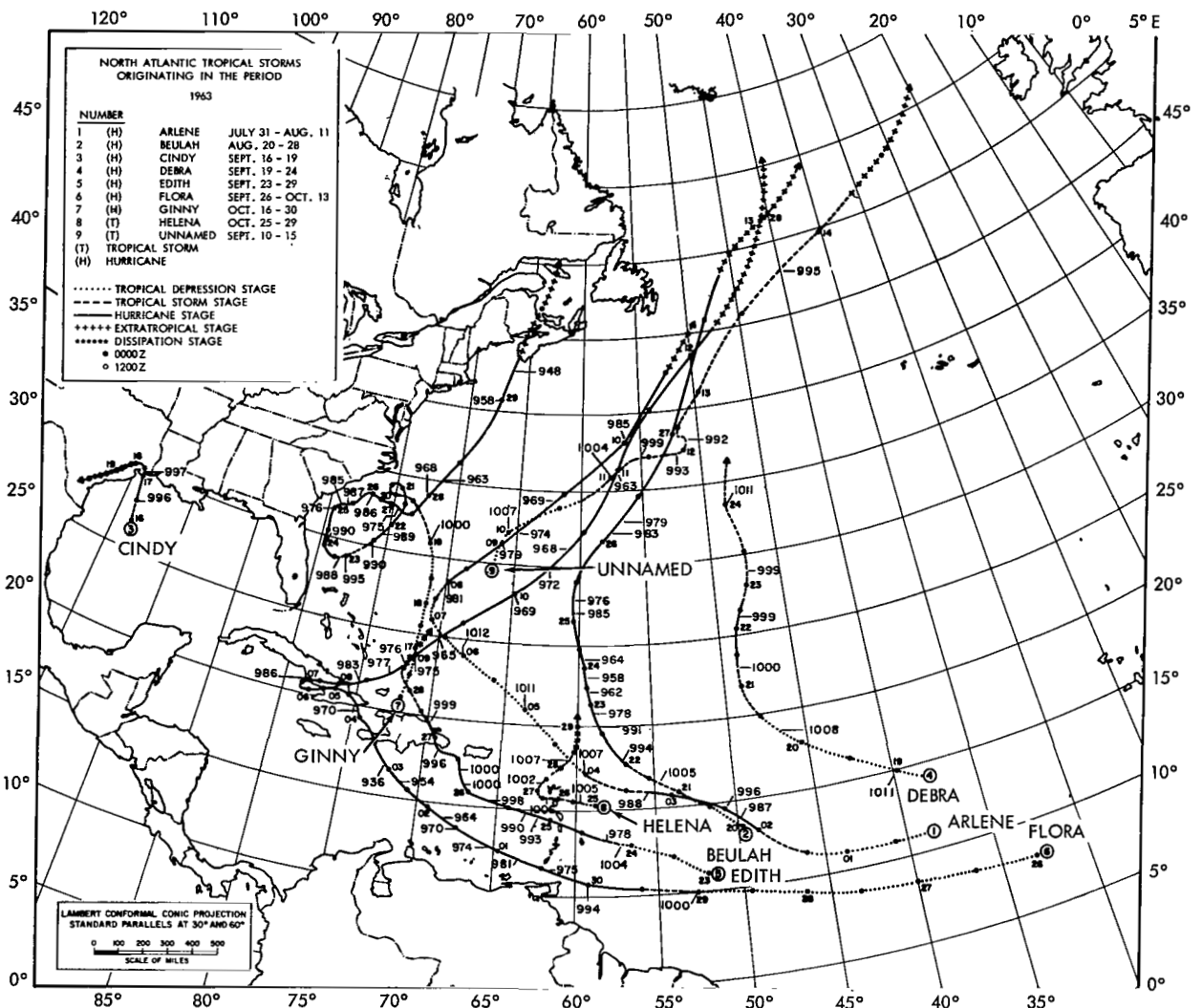


Figure 1—Storm tracks of the 1963 North Atlantic hurricane season. The central pressure (mb) is indicated along the track.

maximum cloud structure detail and still remained a workable chart size. The three possible earth scanning patterns of the Tiros radiometer are the single open, alternating open and closed mode. For the reader who may not be familiar with these modes, a discussion may be found in References 10, 11, 12 and 13. Since there may be significant location errors in closed mode and alternating mode data, notation of all modes analyzed are presented in Table 1. Twenty to ninety grid print maps were run for each storm but only a small proportion of useable data was obtained. The loss of data was caused by a clutch slippage of the satellite tape recorder during the first five to ten minutes of each orbit, the location of the readout "hole" due to the position of the Wallops Island ground station, and insufficient radiation coverage over individual hurricanes (References 10 and 11). The grid print maps were analyzed in terms of uncorrected isotherms of equivalent blackbody temperature T_{BB} in °K. The estimated short-term relative accuracy of the Channel 2 T_{BB} measurements for a given side was 2°K and the absolute accuracy was 5°K. Estimated degradation corrections are shown in Figure 2 which were extracted from References 10 and 11. The definition of effective radiation

Table 1
 Tiros VII Radiation Data Documentation of the 1963 Hurricane Season

Storm	Dates (1963)	Number of Orbits		Readout Number* of Orbits	
		Reduced to FMR Tape Format	Containing Storm Data	Containing Partial Storm Coverage	Containing Maximum Storm Coverage
Arlene	7/31-8/11	48	2	729	744(CM)
Beulah	8/19-8/28	59	5	1036, 1040	910(AM), 925(AM), 1026(OM)
Cindy	9/15-9/18	21	5	1306	1299(OM), 1314(OM), 1328(OM), 1343(OM)
Debra	9/17-9/24	31	1		1362(CM)
Edith	9/23-9/29	34	2		1473(OM), 1480(OM)
Flora	9/28-10/10	76	4	1523, 1546, 1634	1553(OM)
Ginny	10/14-10/30	96	11	1736, 1780, 1786, 1794, 1801, 1868, 1912, 1946	1903(OM), 1926(OM), 1932(OM)
Helena	10/25-10/29	37	4	1961, 1888	1903(OM), 1932(OM)

*Radiometer Scanning Mode:

(OM)—single open mode

(CM)—closed mode

(AM)—alternating mode

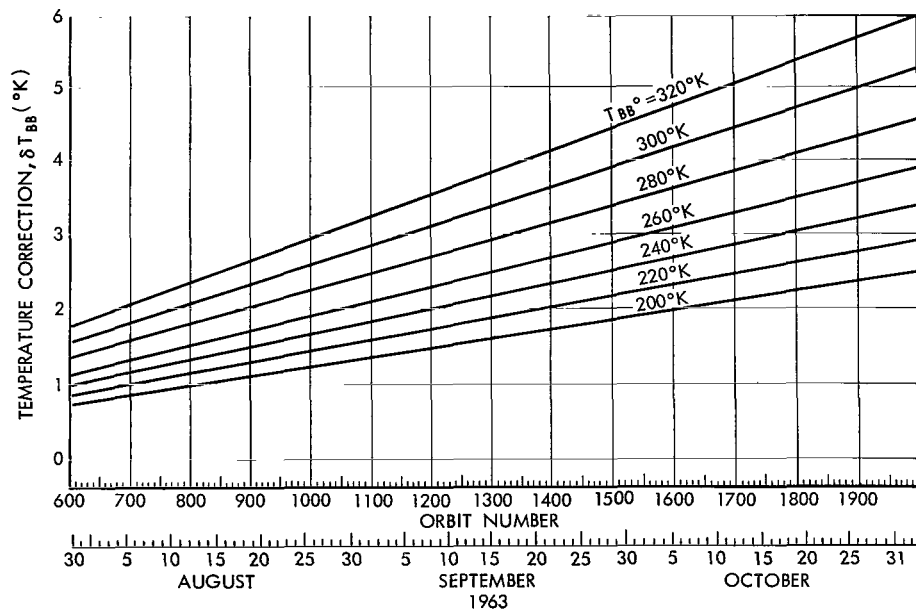


Figure 2—Degradation Correction Nomogram for Channel 2 (8-12 μ), both sides for Tiros VII, orbits 600-2000, 30 July - 2 November 1963. The equivalent blackbody temperature measurement (T_{BB}) should be corrected by adding the δT_{BB} value corresponding to the appropriate orbit number. For example, a measured T_{BB} value of 240°K during orbit 1200 should be increased by 2°K, to correct for instrumental degradation.

height as used in this study is that height in the atmosphere where the ambient temperature equals the equivalent blackbody temperature. By using radiosonde data in close proximity to the hurricane position, an estimation of the effective radiation height of the storm's clouds may be determined. The cloud top heights add a vertical dimension to the horizontal structure of the storm which will become increasingly valuable for military and civilian flights and for meteorological research in studies such as vertical motion, cyclogenesis, thunderstorm and tornado research, and cloud seeding.

The aerial reconnaissance data nearest in time to the corresponding seventeen grid print maps is contained in Table 2. All center of circulation or eye positions in this table were checked for correlation with the Tiros VII radiation analyses and found in good agreement with the main cloud features.














Table 2
Summary of Tiros VII 8-12 μ Radiation Data Presented in Map Form
and the Corresponding Aerial Reconnaissance Data

Tiros VII Radiation Data					Aerial Reconnaissance Reports			
Figure	Storm	Orbit	Date - 1963	Time (Z)	Approximate Minimum T ($^{\circ}$ K)	Time (Z)	Lat.-Long.	Max. Surface Wind Speed (knots)
3	Arlene	744	Aug. 8	1744	215	1800	28.8 $^{\circ}$ N-69.1 $^{\circ}$ W	65
6	Beulah	910	Aug. 19	2213	210	----	-----	--
7	Beulah	925	Aug. 20	2232	220	2200	14.7 $^{\circ}$ N-51.3 $^{\circ}$ W	25
10	Beulah	1026	Aug. 27	1822	220	1800	41.6 $^{\circ}$ N-51.0 $^{\circ}$ W	70
12	Cindy	1299	Sept. 15	0645	205	----	-----	--
13	Cindy	1314	Sept. 16	0705	205	1200	26.7 $^{\circ}$ N-93.7 $^{\circ}$ W	35
14	Cindy	1328	Sept. 17	0548	210	0600	28.7 $^{\circ}$ N-94.2 $^{\circ}$ W	55
16	Cindy	1343	Sept. 18	0610	235	0600	30.1 $^{\circ}$ N-94.9 $^{\circ}$ W	35
20	Debra	1362	Sept. 19	1202	235	1200	15.0 $^{\circ}$ N-39.8 $^{\circ}$ W	30
22	Edith	1473	Sept. 27	0114	225	0000	17.8 $^{\circ}$ N-67.5 $^{\circ}$ W	70
23(b)	Edith	1480	Sept. 27	1137	220	1200	18.7 $^{\circ}$ N-69.3 $^{\circ}$ W	55
27	Flora	1553	Oct. 2	1004	205	1000	14.5 $^{\circ}$ N-69.0 $^{\circ}$ W	125
31	Ginny	1903	Oct. 26	0211	220	0400	32.9 $^{\circ}$ N-77.5 $^{\circ}$ W	85
34	Ginny	1926	Oct. 27	1645	225	1600	32.8 $^{\circ}$ N-74.9 $^{\circ}$ W	70
36	Ginny	1932	Oct. 28	0119	220	0000	32.6 $^{\circ}$ N-73.4 $^{\circ}$ W	75
42	Helena	1903	Oct. 26	0220	200	0000	15.4 $^{\circ}$ N-60.1 $^{\circ}$ W	40
45	Helena	1932	Oct. 28	0123	205	0000	16.9 $^{\circ}$ N-61.9 $^{\circ}$ W	35

The definitions of the four stages of hurricane development used in this study are in accordance with Dunn and Miller (Reference 14) as follows:

1. Tropical Disturbance - Rotary circulation slight or absent at the surface but possibly better developed aloft. There are no closed isobars and no strong winds.
2. Tropical Depression - One or more closed surface isobars. Wind force equal to or less than 33 knots.

Table 3
Tiros Nephanalysis Symbols

TERM	SYMBOL	TERM	SYMBOL	TERM	SYMBOL
Major Boundary		Overcast		CUFM (Cumuloform)	
Minor Boundary		Heavy		CIFM (Cirroform)	
Clear	CLR	Thin		CB (Cumulonimbus)	
Scattered	S	Variable		Bands	
Broken	B 	STFM (Stratoform)		Vortex	

3. Tropical Storm - Closed surface isobars, wind force 34 to 63 knots.
4. Hurricane - Wind force 64 knots or more.

The symbols used in the hurricane nephanalyses in accordance with the National Weather Satellite Center definitions, prior to 3 January 1964 are illustrated in Table 3.

THE 1963 NORTH ATLANTIC HURRICANE SEASON

Hurricane Arlene

Arlene was detected in the tropical depression stage by Tiros VI in the subtropical Atlantic on 31 July 1963. It moved on a westerly track and intensified to hurricane stage (85 knots) by 1 August. By the night of 3 August, it had weakened to a tropical depression with winds less than 25 knots. For the period 5-7 August, Arlene remained a tropical depression but by 1600 Z, 8 August, it had reintensified to hurricane stage and commenced recurvature to the northeast (Figure 1).

A Tiros VII radiation analysis for the period 1744-1751 Z, 8 August is shown in Figure 3 and the corresponding nephanalysis and mosaic is shown in Figure 4. The intense middle and high clouds of the hurricane are outlined by the 260 and 230°K isotherms respectively. Minimum T_{BB} values of 215 to 220°K are in the area of the reported eye location, 28.8°N, 69.1°W (Table 2). The T_{BB} value of 215°K in Figure 3 should be increased by 1°K from Figure 2, to yield a corrected value of 216°K. This would lower the effective radiation height of the high clouds from 12 to 11.9 km. Clear to scattered clouds are outlined by the 275 to 280°K isotherms. As an example of fine detail, a small warm region (240°K) at 28-29°N, 69-71°W in Figure 3 is seen as a break in the cloud canopy in the TV insert, in Figure 4. The comparative location accuracy of small cloud features by the television and radiation systems was found to be ± 1 to 1.5°. The mass of cloudiness to the northwest of the hurricane was identified as an open wave which is shown on the 1800 Z, 8 August surface chart, Figure 5. Figures 3, 4 and 5 show excellent agreement between the synoptic analysis, radiation analysis and the television pictures in defining the location and pattern of hurricane cloudiness. In addition, the radiation analysis contains a three dimensional character which directly complements the television pictures. The eye of Hurricane Arlene passed over Bermuda.

at 1600 Z, 9 August, where a maximum surface wind of 84 knots was recorded. The storm finally lost its tropical characteristics by 10-11 August 1963, when it merged with a polar front in the North Atlantic.

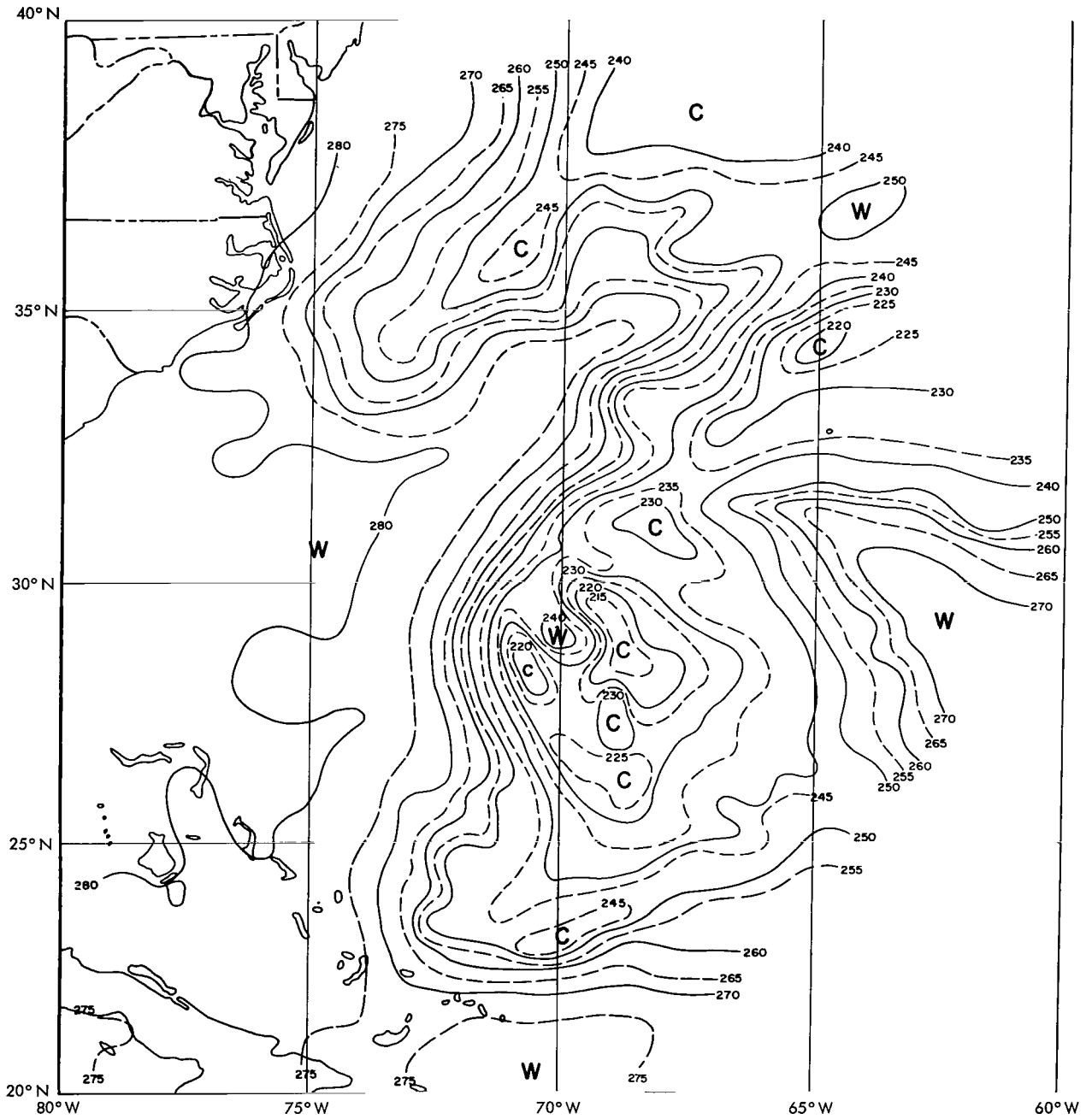


Figure 3—Channel 2 radiation analysis indicating Hurricane Arlene, 1744-1751Z, 8 August 1963, orbit 744. The isolines show T_{BB} values in $^{\circ}K$ (uncorrected for instrumental degradation).

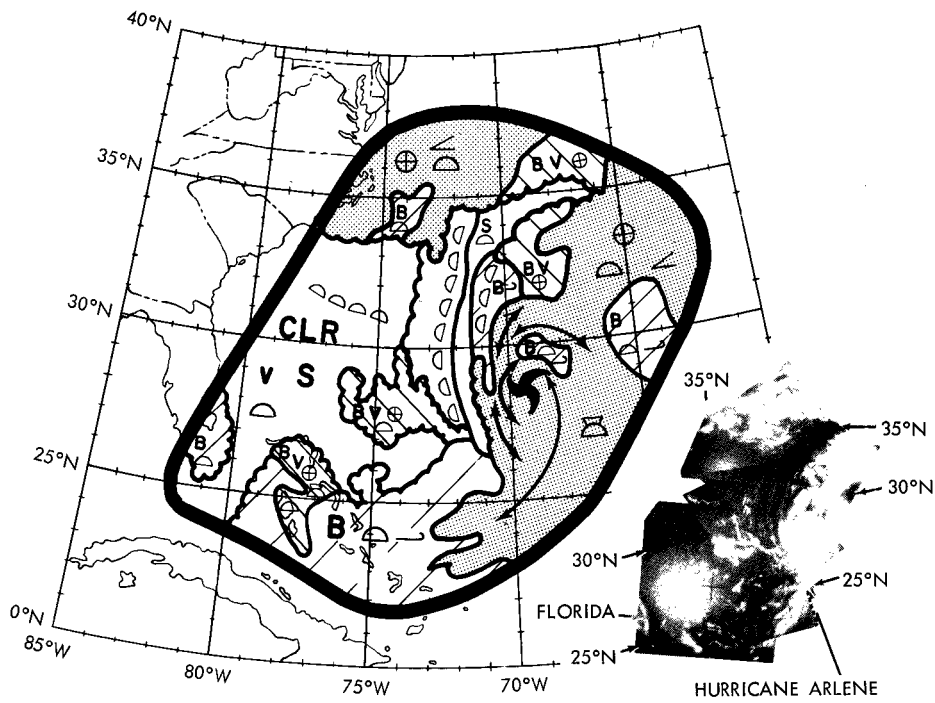
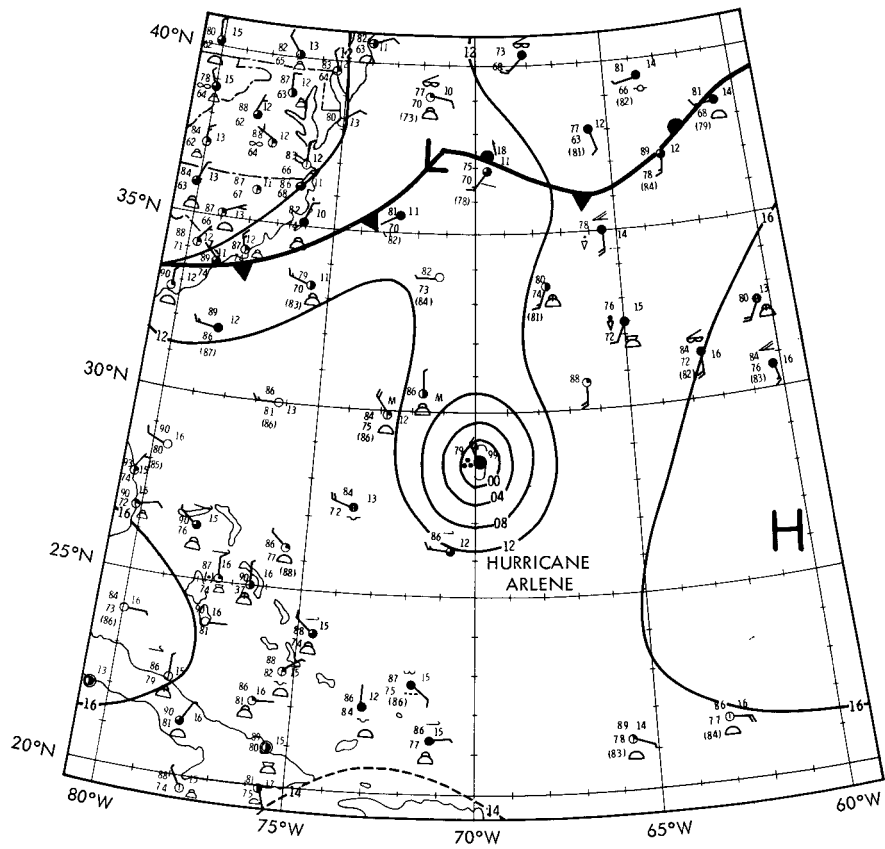


Figure 4—Mosaic and neph-analysis of Tiros VII television pictures indicating Hurricane Arlene, 1749 Z, 8 August 1963, orbit 744.

Figure 5—Surface synoptic chart, 1800 Z, 8 August 1963, indicating Hurricane Arlene (National Meteorological Center, U. S. Weather Bureau).



Hurricane Beulah

The tropical disturbance that developed into Hurricane Beulah apparently formed on the Intertropical Zone of Convergence (ITC) during a period of unusual northward displacement. U.S. Navy aircraft reconnaissance reports indicated masses of broken, weak to moderate radar echoes within the area bounded by 10 to 15°N and 45 to 50°W, at 1500 to 1700 Z on 19 August 1963. Surface winds of 20 knots, 1008 mb surface pressure, and cloud tops averaging 30,000 ft (9.1 km) with maximum tops 37,000 ft (11.3 km) were recorded but no pattern of cyclonic circulation was detected.

The radiation analysis of Beulah at 2213 Z on this date is shown in Figure 6. The cold T values of 210 to 215°K relate to the effective radiation cloud heights respectively of 13 to 12.5 km (0.1 km lower when corrected for degradation). Since there was a five to seven hour time differential between aircraft and satellite reports, the 1 to 4 km cloud height difference between the two observations can be reasonably explained by accelerated storm development. The storm exhibited a singular disorganization in its cloud fields and a lack of circulation center which is typical of a tropical disturbance (Reference 15). Five high cloud areas with T_{BB} values of 210 to 235°K appear to be arranged unsymmetrically within the area bounded by 8 to 15°N, 45 to 50°W.

Continued aerial reconnaissance on 20 August reported moderate to strong lines of radar echoes within the area bounded by 10 to 18°N and 49 to 58°W at 1300 to 1700 Z. Surface winds of 30 knots, 1006 mb surface pressure and multi-layered clouds, tops averaging 25,000 to 35,000 ft (7.6 to 10.7 km) with maximum tops 45,000 ft (13.7 km) were indicated, however, no definite circulation pattern nor eye was found.

Beulah in its early tropical depression stage at 2232 Z on 20 August is outlined in Figure 7. The cold T_{BB} values of 220 to 225°K

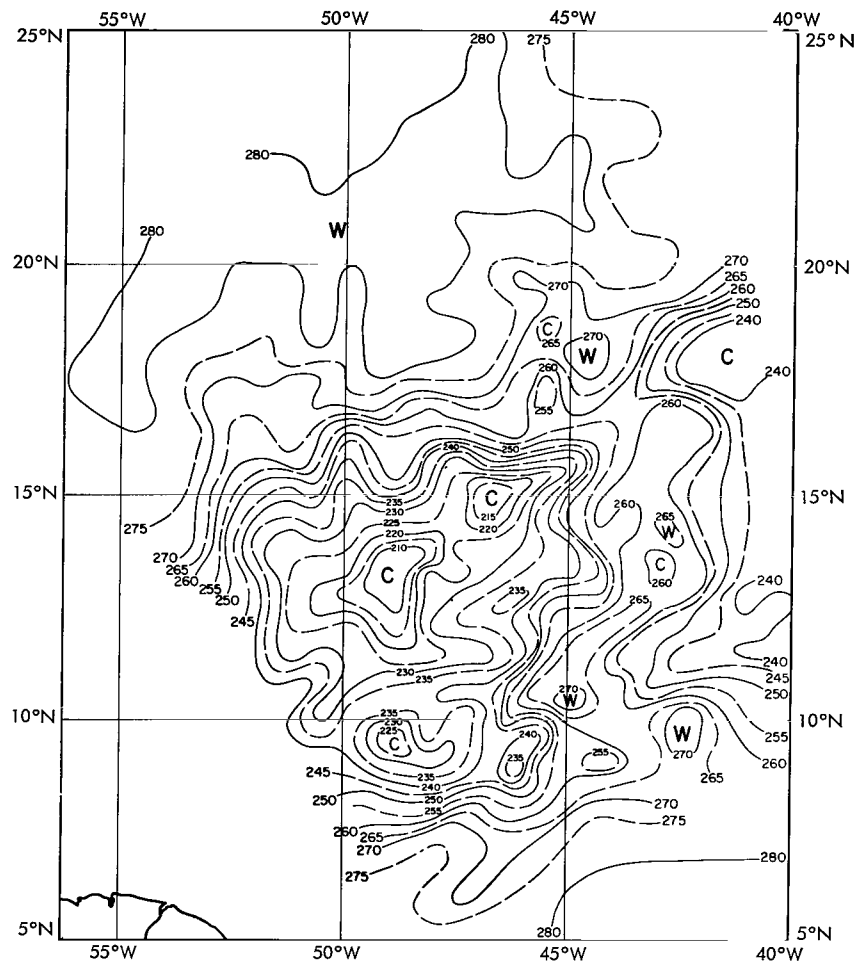


Figure 6—Channel 2 radiation analysis indicating Tropical Disturbance Beulah, 2213–2220 Z, 19 August 1963, orbit 910. The isolines show T_{BB} values in °K (uncorrected for instrumental degradation).

relate to the effective radiation cloud heights respectively of 12.5 to 11.5 km (0.2 km lower when corrected for degradation). The storm developed a more centralized cirroform cloud canopy (220 to 235 °K) which appears to be 1 to 2 km lower in altitude than on 19 August (Figure 6). In addition, a pronounced line of intensive CB cloud cells can be seen along the south, west and north perimeter of the storm. Tiros VII television pictures of Beulah were taken during its tropical storm stage at 1101 Z on 21 August, as shown in Figure 8. Anticyclonic flow at 200 mbs was well established by 1800 Z, 21 August, and a steady intensification had begun over the storm, near the edge of the ITC.

At 1255 Z on 22 August, a U.S. Navy reconnaissance plane located a well-defined eye 25 miles in diameter at 18° 08'N, 57° 26'W. Maximum surface winds of 60 knots and central minimum

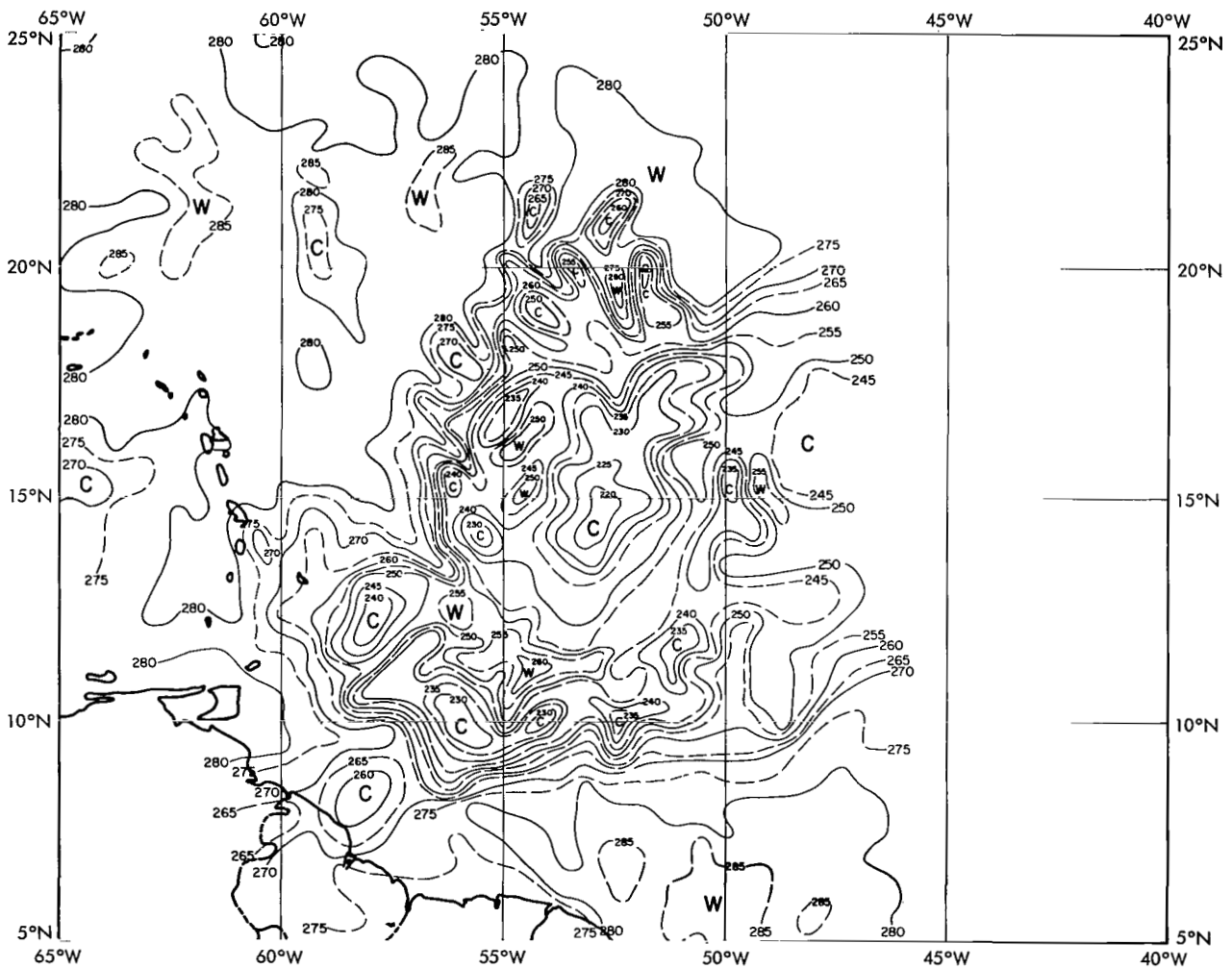


Figure 7—Channel 2 radiation analysis indicating Tropical Depression Beulah, 2232-2239 Z, 20 August 1963, orbit 925. The isolines show T_{BB} values in °K (uncorrected for instrumental degradation).

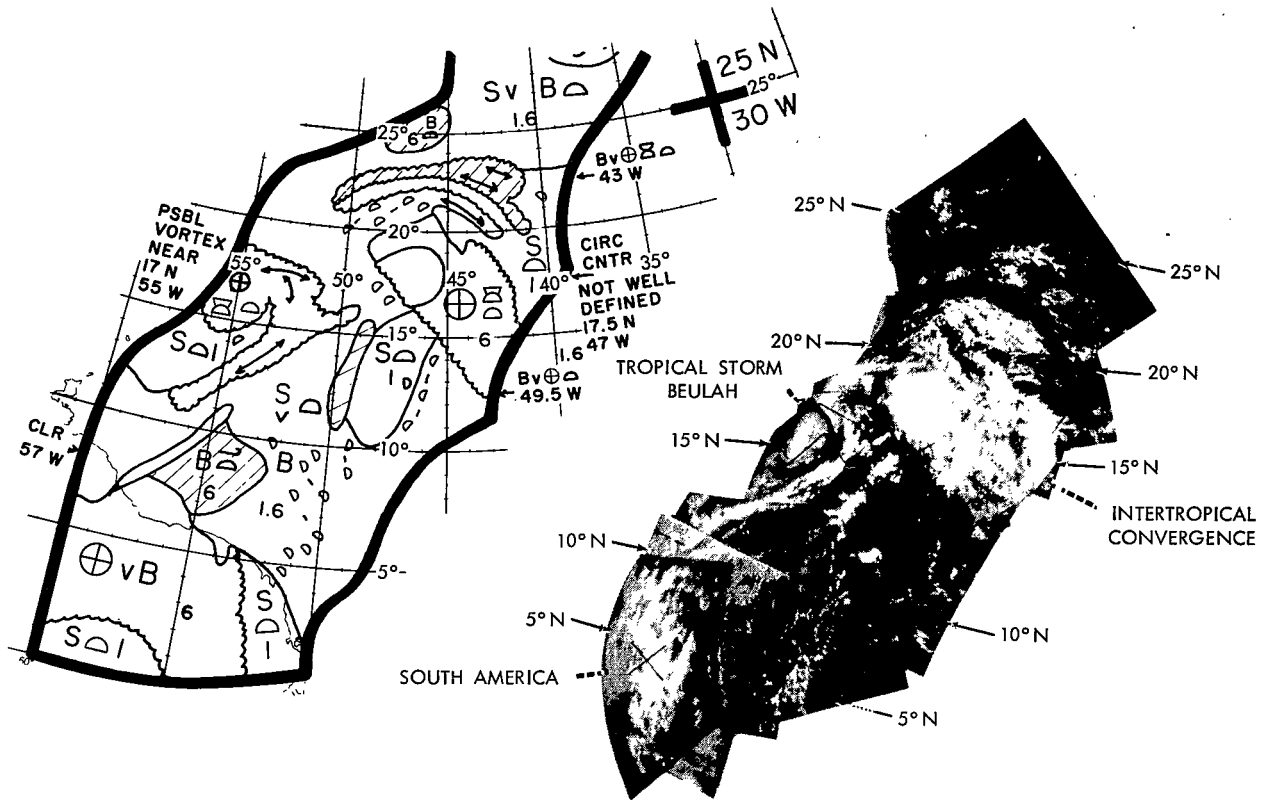


Figure 8—Mosaic and nephanalysis of Tiros VII television pictures indicating Tropical Storm Beulah, 1101 Z, 21 August 1963, orbit 932 (reacout 934 accuracy $\pm 2^\circ$).

surface pressure of 994 mb were reported. Figure 9 shows the Tiros VII television coverage over Beulah at approximately the same time. The eye appears centered under the circular cloud canopy while the expanding cloud shield extending far to the NE of the center of circulation, suggests a rapidly intensifying condition.

Two experimental cloud seeding experiments over Beulah were conducted by the U.S. Weather Bureau, National Hurricane Research Laboratory, during Project Stormfury on 23-24 August 1963. Approximately 800 lbs of silver iodide smoke were dispersed into the clouds surrounding the eye during these two days. Some variation in the eye wall clouds and wind field was noted by monitoring research aircraft but no definite conclusions on the effect of the experimental cloud seeding was reached (Reference 16).

Maximum surface winds of 105 knots and minimum surface pressure of 958 mb within Beulah were reported by aircraft on 0630 Z on 24 August. Under the influence of a trough in the westerlies, Beulah began to deteriorate and accelerate to the northeast. On 27 August, the storm passed within 250 miles SE of Newfoundland, moving NNE at 35 kts.

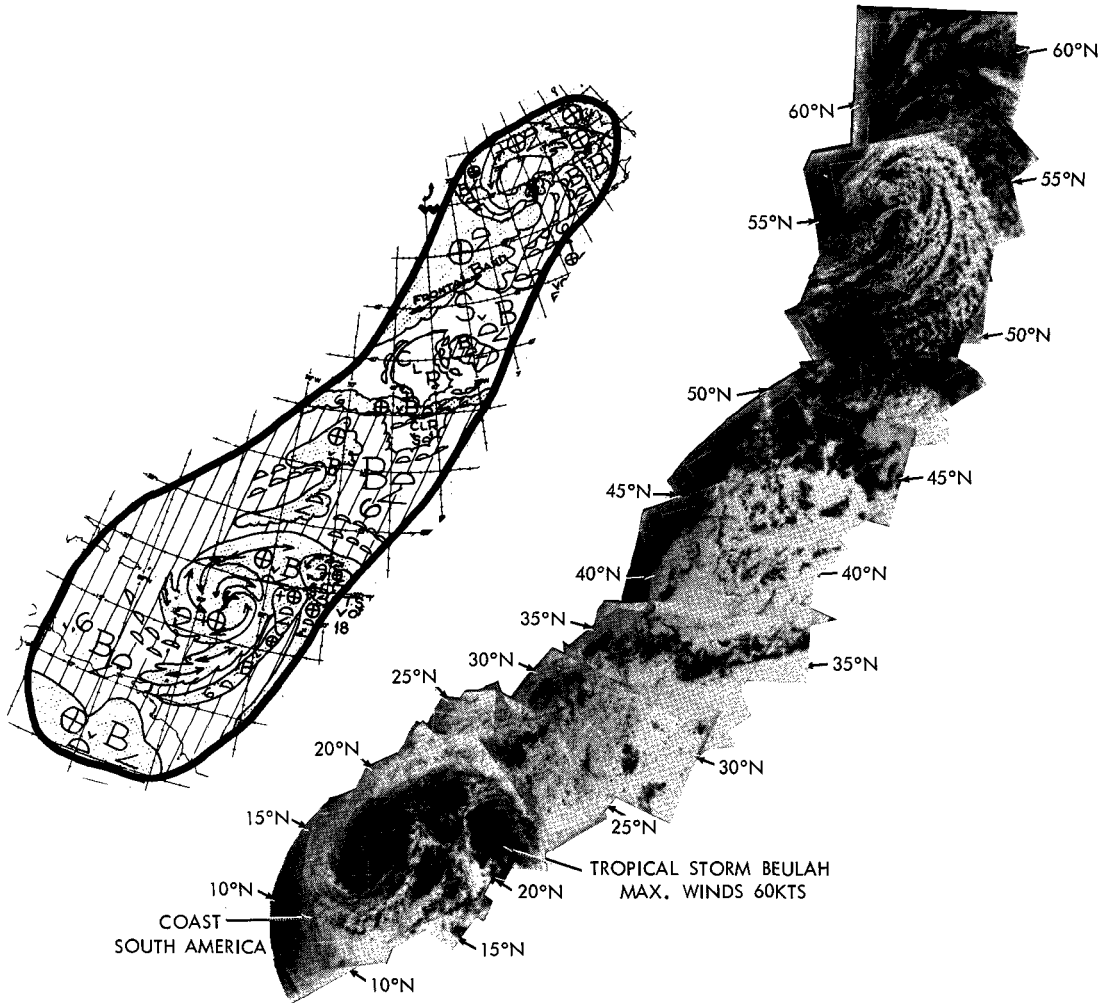


Figure 9—Mosaic and nephanalysis of Tiros VII television pictures indicating Tropical Storm Beulah, 1125 Z, 22 August 1963, orbit 947 (readout 948 accuracy $\pm 1.5^\circ$).

A Tiros VII radiation analysis over Beulah at 1822 Z on 27 August, in this region is shown in Figure 10. At this time Beulah was becoming an extratropical storm (70 knots surface winds) as it encountered the cold waters of the North Atlantic. The cold T_{BB} values of 220 to 225°K over Beulah and the frontal zone relate to the effective radiation cloud heights respectively of 12 to 11 km (0.2 km lower when corrected for degradation). This radiation analysis outlines the last stages of Beulah and the elongated clouds of the open wave, SE of Newfoundland. The synoptic events depicted by the radiation data are shown on the surface map in Figure 11.

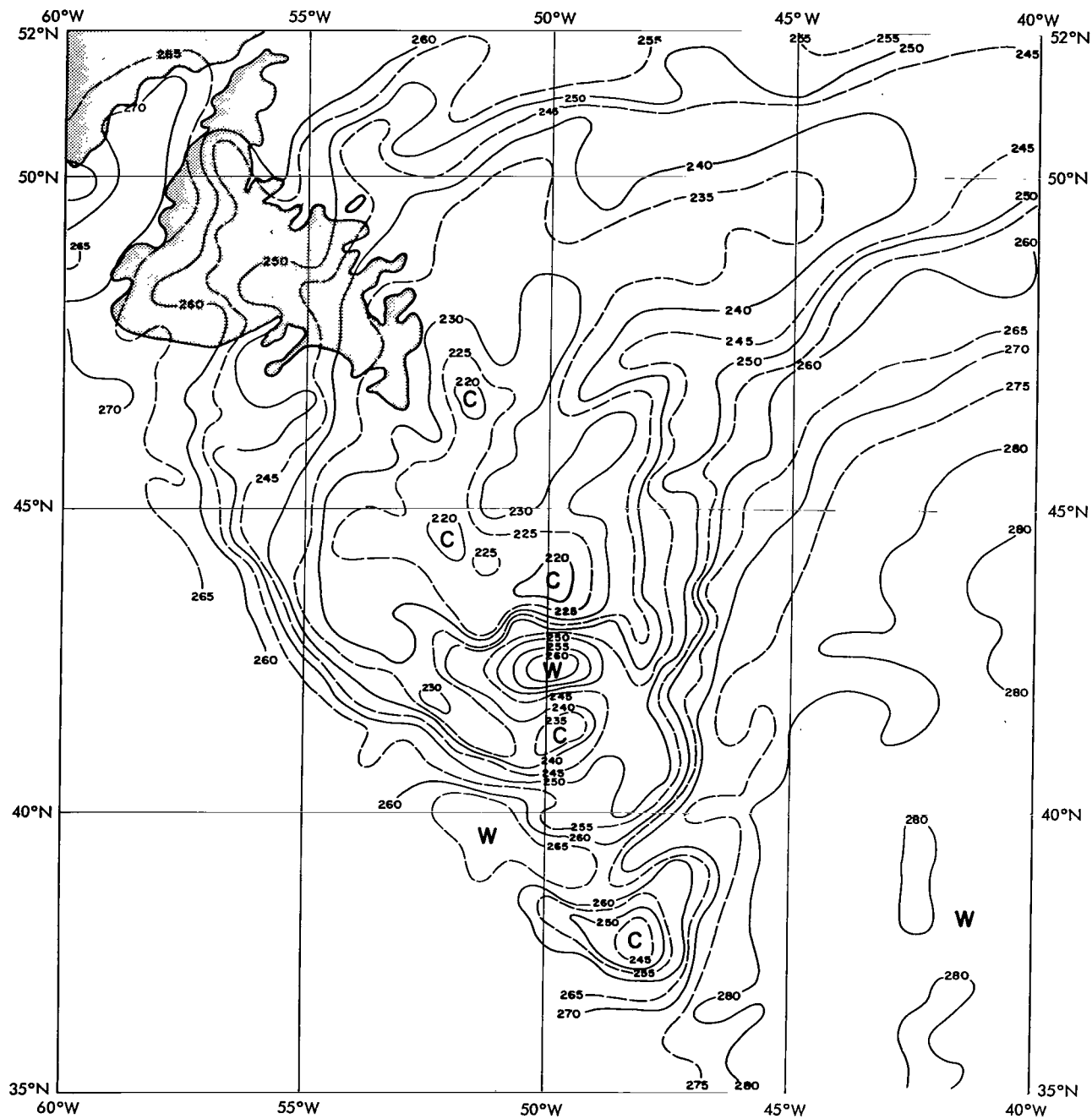


Figure 10—Channel 2 radiation analysis indicating Hurricane Beulah, 1822-1829 Z, 27 August 1963, orbit 1026. The isolines show T_{BB} values in $^{\circ}K$ (uncorrected for instrumental degradation).

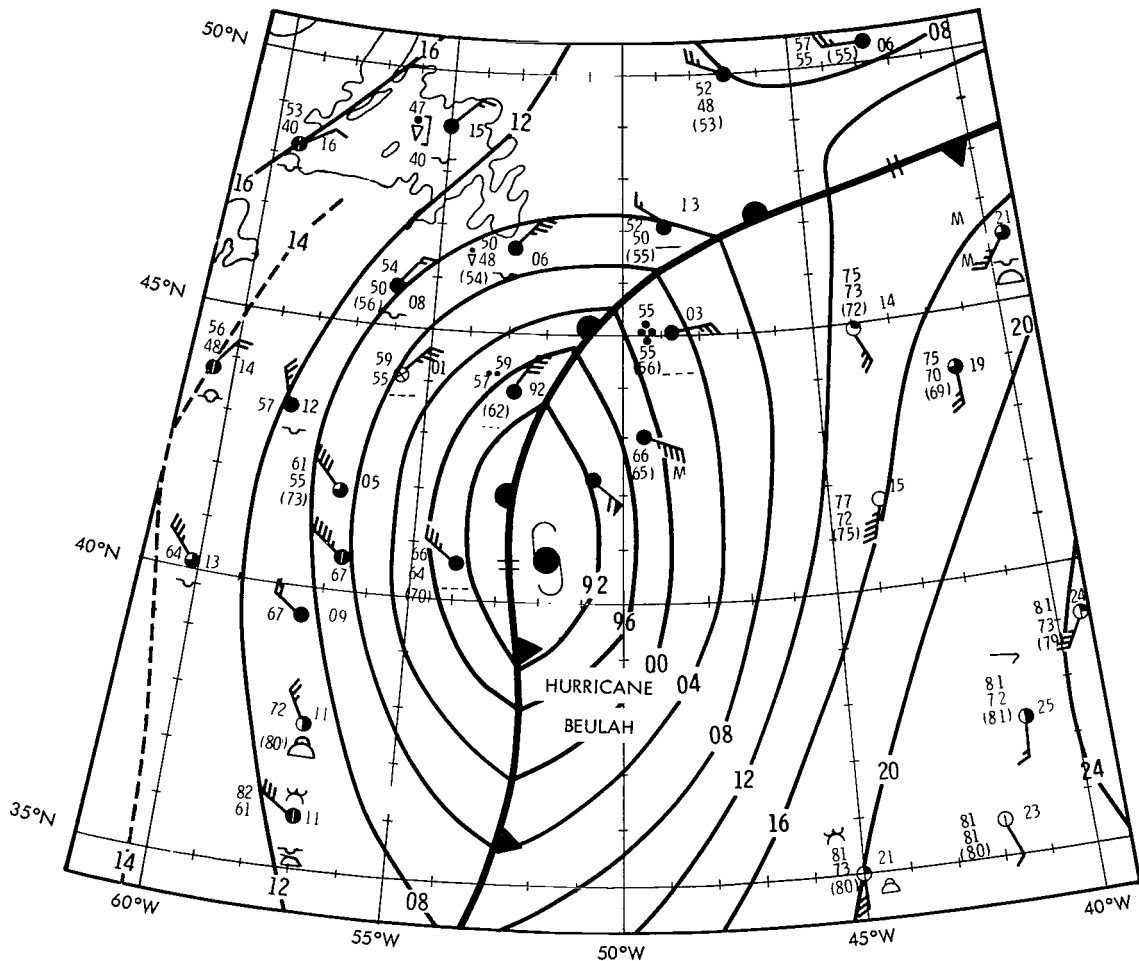


Figure 11—Surface synoptic chart, 1800 Z, 27 August 1963 indicating Hurricane Beulah (National Meteorological Center, U.S. Weather Bureau).

Hurricane Cindy

Hurricane Cindy, the third and most short-lived storm of the 1963 season, formed on the trailing edge of a surface quasi-stationary front and an upper trough in the western Gulf of Mexico on 16 September 1963 (Reference 17). Weather conditions had been disturbed for several days in the southwestern Gulf of Mexico. Ship reports had indicated that a tropical storm had formed and was intensifying rapidly on 15 September.

Tiros VII radiation data over Cindy in its early formative stage at 0645 Z on 15 September are shown in Figure 12. The main outline of the small storm is shown within the area bounded by 20 to 25°N and 90 to 95°W. The cold T_{BB} values, 205 to 210°K relate to effective radiation cloud heights respectively of 14.5 to 13.5 km (0.1 km lower when corrected for degradation). Several other widely distributed cloud systems (205 to 250°K) are shown over Central America

and the northeastern Gulf of Mexico. The storm appears to be well organized and slightly elliptical in shape with two smaller cloud regions along the NW edge.

Investigative aerial flights on 16 September at 19 to 23 Z reported cloud tops averaging 28,000 ft (8.5 km) with maximum tops of 50,000 ft (15.2 km) within the storm area. The eye was indicated as being poorly defined with a maximum observed surface wind of 55 knots and a minimum surface pressure of 996 mb.

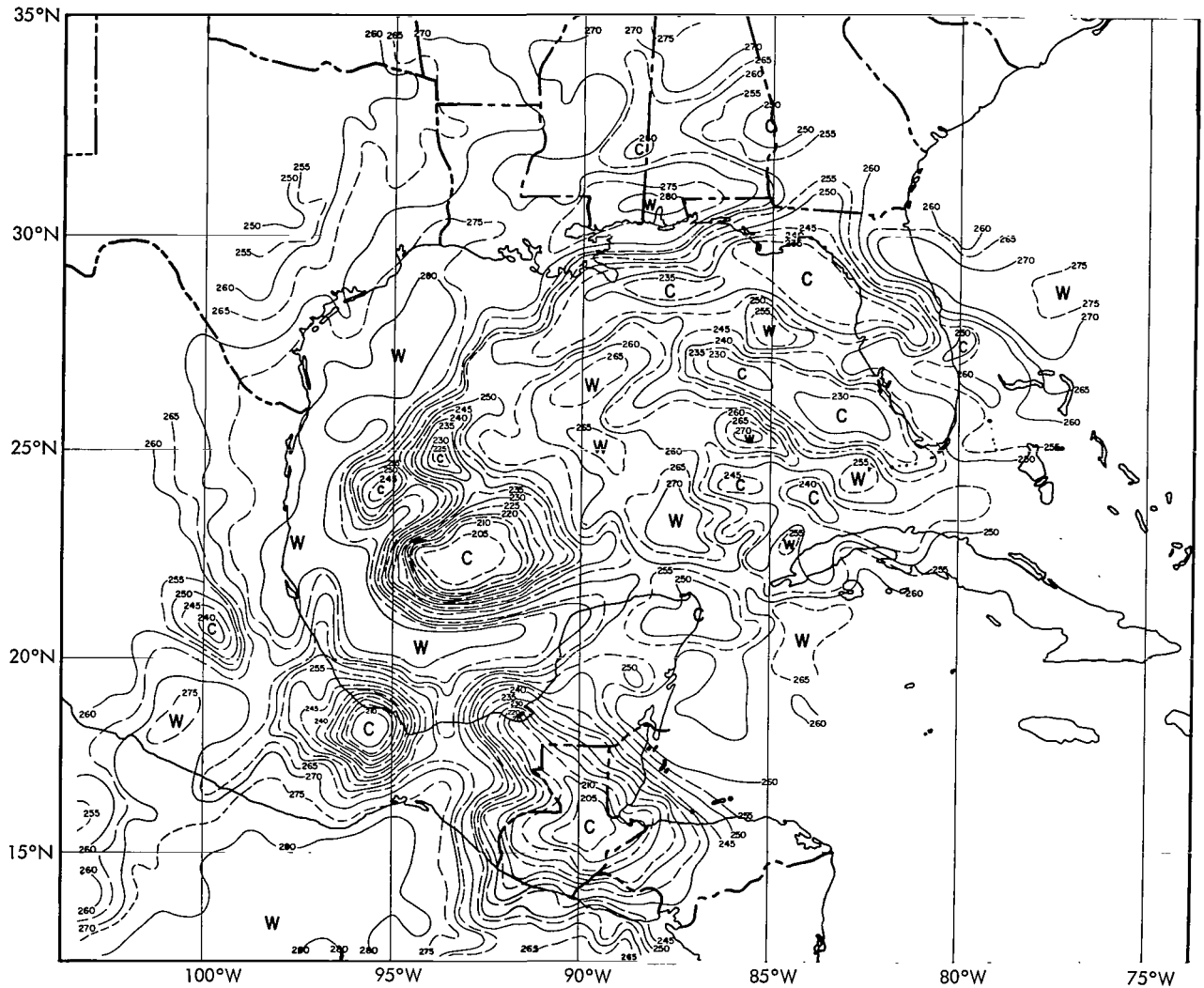


Figure 12—Channel 2 radiation analysis indicating the formative stage of Cindy, 0645–0653 Z, 15 September 1963, orbit 1299. The isolines show T_{BB} value in $^{\circ}\text{K}$ (uncorrected for instrumental degradation).

Cindy is shown in its tropical storm stage by Tiros VII radiation data at 0705 Z on 16 September, Figure 13. The high cloud area outlined by the 235°K isotherm has enlarged and become more circular in shape. The cloud top temperatures (205 to 210°K) remained the same on 15 and 16 September; hence, the effective radiation cloud heights of 14.2 to 13.8 km were essentially unchanged. The less cloudy coastal and Gulf region to the west and southeast of the storm has increased in size as Cindy moved northward to the Texas coast.

Tiros VII radiation data was available (Figure 14) at 0548 Z on 17 September and outlined a comma-shaped cloud structure with a tail-like cloud (260 to 275°K) extending southward into the

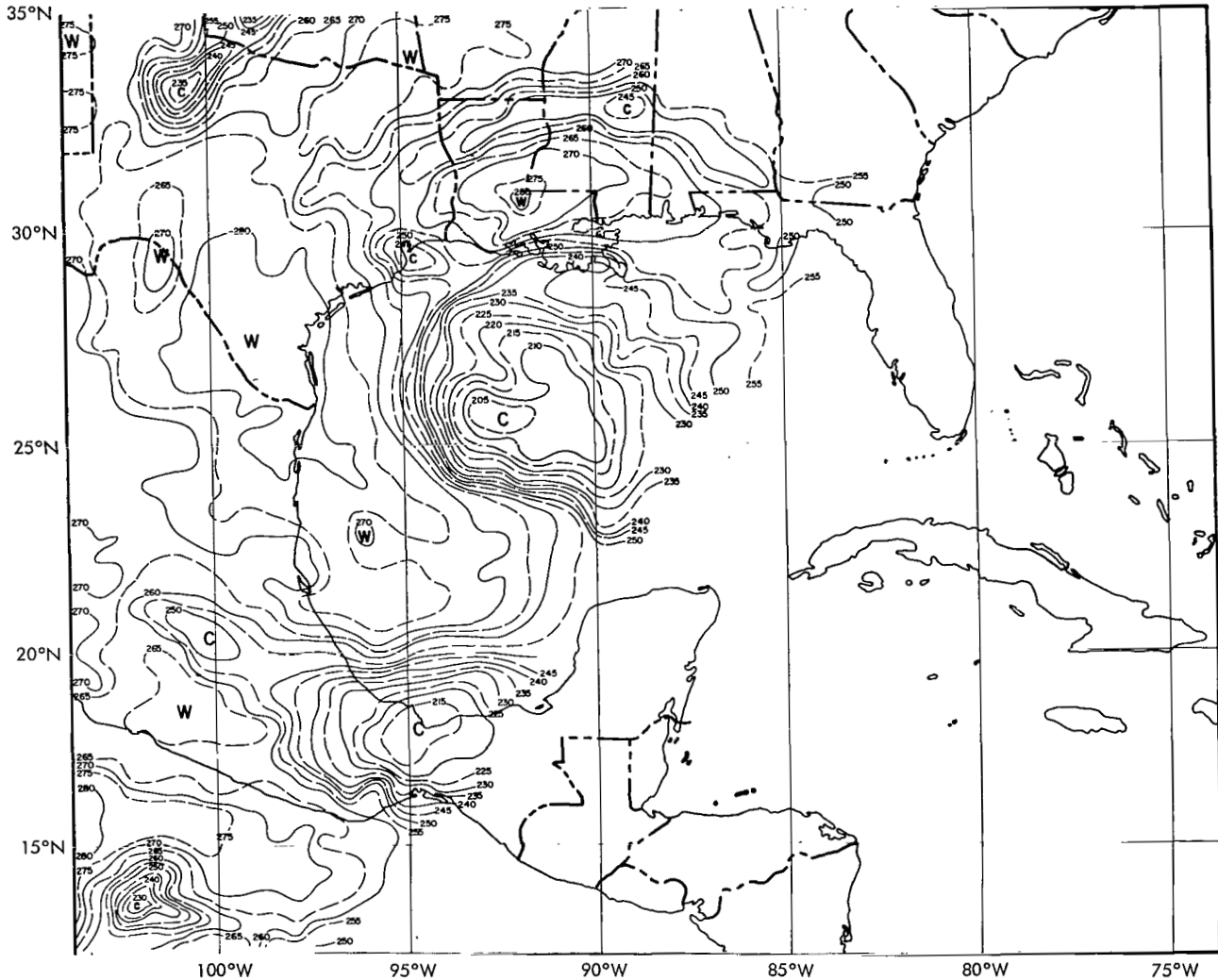


Figure 13—Channel 2 radiation analysis indicating Tropical Storm Cindy, 0705–0713 Z, 16 September 1963, orbit 1314. The isolines show T_{BB} values in °K (uncorrected for instrumental degradation).

central Gulf of Mexico. Two smaller (210 to 220°K) T_{BB} cloud canopy centers along 28°N, between 90 to 95°W relate to the effective radiation cloud heights respectively of 14 to 12 km (0.1 to 0.2 km lower when corrected for degradation). It can be noted that the central cloud T_{BB} values have warmed hence the effective radiation cloud heights have lowered since 16 September. Several other cold cloud shields may be seen over Mexico, Central America, and the Caribbean Sea. The cold T_{BB} values analyzed over the Bahamas and east-central Florida relate to the cloudy stationary front in that area as shown on the surface map in Figure 15. A radar photograph of Cindy from a WSR-57 radar at Galveston at 0950 Z on 17 September shows the storm's cloud structure in some detail (inset, Figure 14). The 100 mile range with 20 mile range markers from

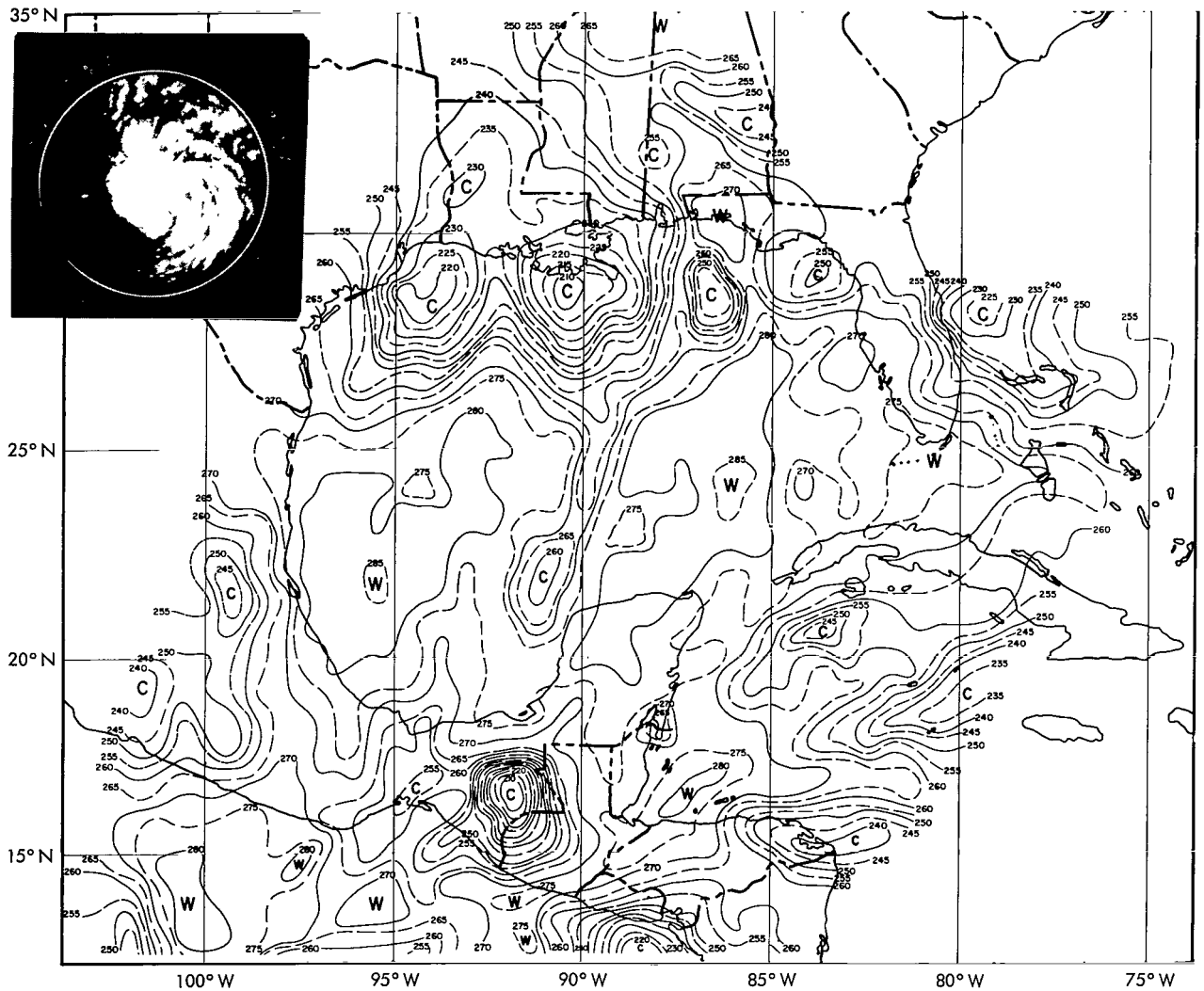


Figure 14-Channel 2 radiation analysis indicating Hurricane Cindy, 0548-0556 Z, 17 September 1963, orbit 1328. The isolines show T_{BB} values in °K (uncorrected for instrumental degradation), WSR-57 radar photograph of Cindy from Galveston, Texas, 0950 Z, 17 September 1963, 100 miles range, 20 mile range markers (Courtesy of U.S. Weather Bureau).

Galveston are shown. The center of the storm was located at $28^{\circ} 51'N$, $94^{\circ} 38'W$ at this time. At 1500 Z, the eye of Hurricane Cindy, about 20 miles in diameter, reached the Gulf coast between Galveston and Port Arthur, Texas. Cindy became stationary for 18 hours after it crossed the east Texas coastline which resulted in an extended period of heavy rainfall, totalling 15 to 20 inches. Cindy is shown at the beginning of its dissipating stage at 0610 Z on 18 September, in Figure 16. The dense cirroform cloud canopy formerly outlined by the 205 to $220^{\circ}K$ isotherms in Figures 12, 13 and 14 has now thinned out or disappeared. Only weakened remnants of middle and lower clouds (235 to $265^{\circ}K$) remain to be detected along the Gulf coast. The decrease of the high cloud canopy occurred coincidentally with diminished outflow aloft and the loss of the storm's source of potential energy. Increased cloud development (cold T_{BB} values) is shown along the Central America-eastern Pacific area, south of $20^{\circ}N$ which could relate to activity along the ITC.

A time section, Figure 17, was drawn for Lake Charles, Louisiana (240) which depicts the synoptic events aloft as Cindy approached the Texas coast. The first indication of outflow from the storm area is shown by an upper shear line which passed Lake Charles on 16 September. The southerly winds over Lake Charles from the 500 to 200 mb level were caused by the peripheral

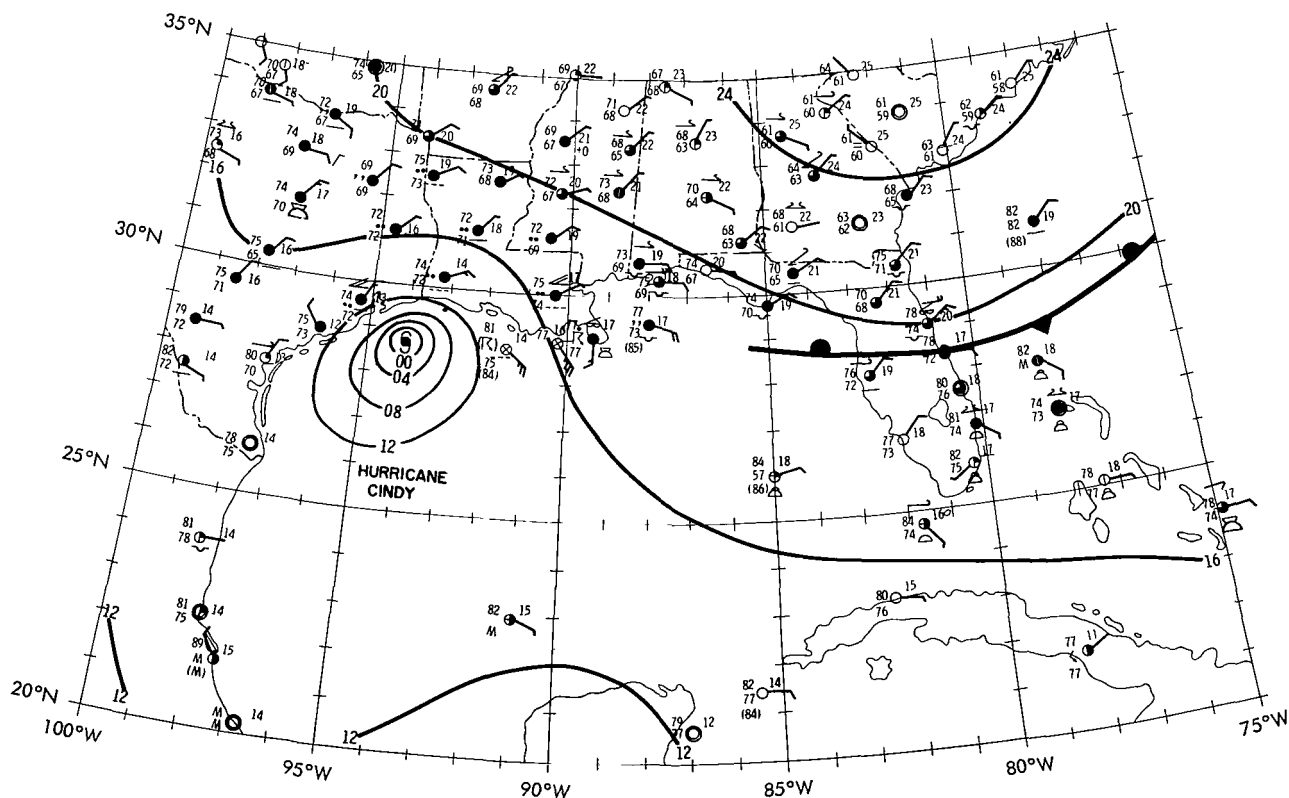


Figure 15-Surface synoptic chart, 0600 Z, 17 September 1963, indicating Hurricane Cindy (National Meteorological Center, U.S. Weather Bureau).

circulation of a strong high aloft which was centered over the Gulf of Mexico. This high moved NW over Hurricane Cindy as it reached the Gulf coast and it settled over central Texas as the decaying storm moved SW towards Houston. The effect of this ridge line movement from 17 to 20 September, is shown by the marked wind shifts aloft from SW to NNE. A pronounced warming of 1 to 2°C/24 hours from 16-18 September identifies the warm core development of the storm in Figure 17, and coincident height rises at upper elevations during this period are an indication of the intense outflow aloft (Reference 18).

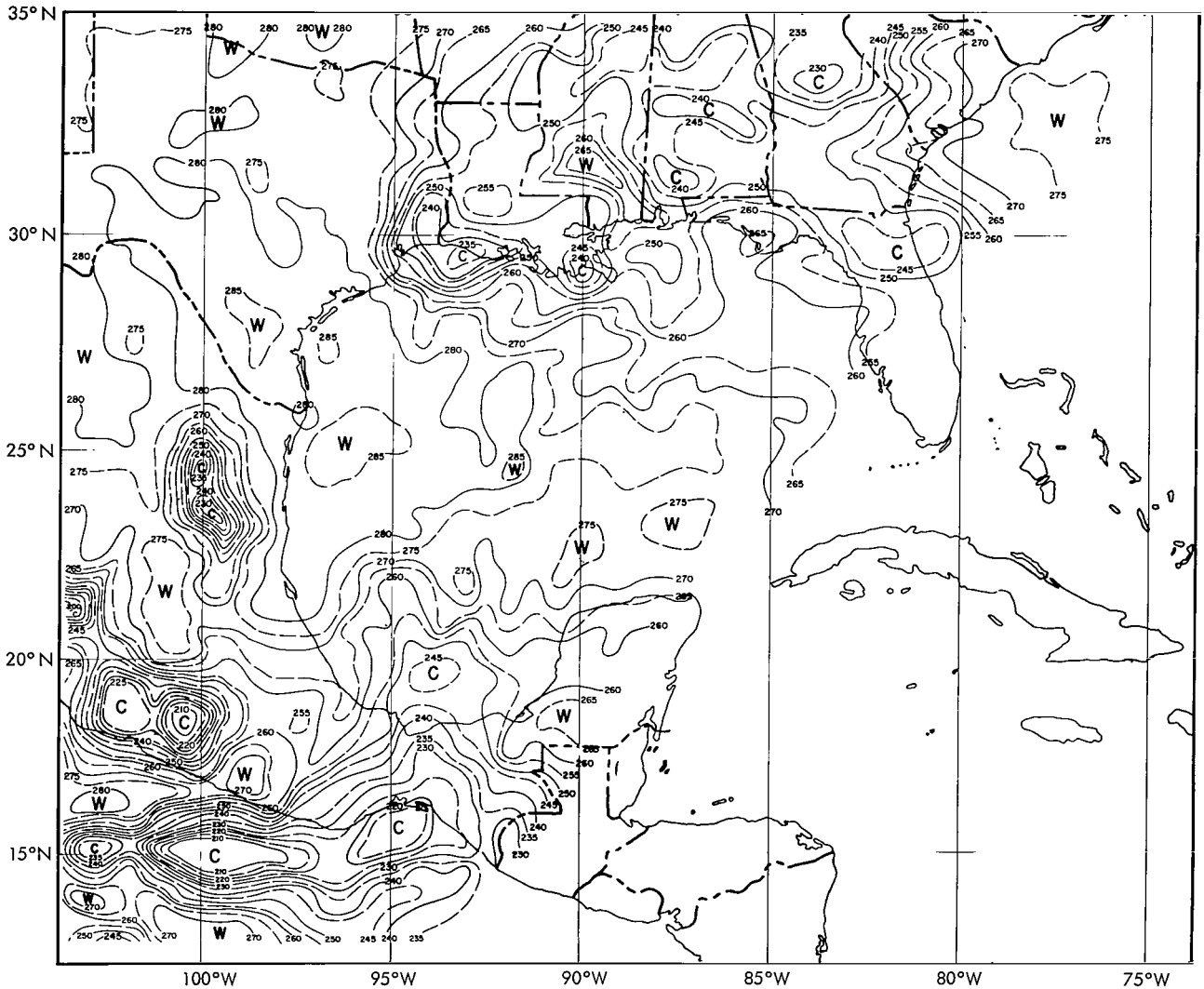


Figure 16—Channel 2 radiation analysis indicating the dissipative stage of Hurricane Cindy, 0610-0618 Z, 18 September 1963, orbit 1343. The isolines show T_{BB} values in °K (uncorrected for instrumental degradation).

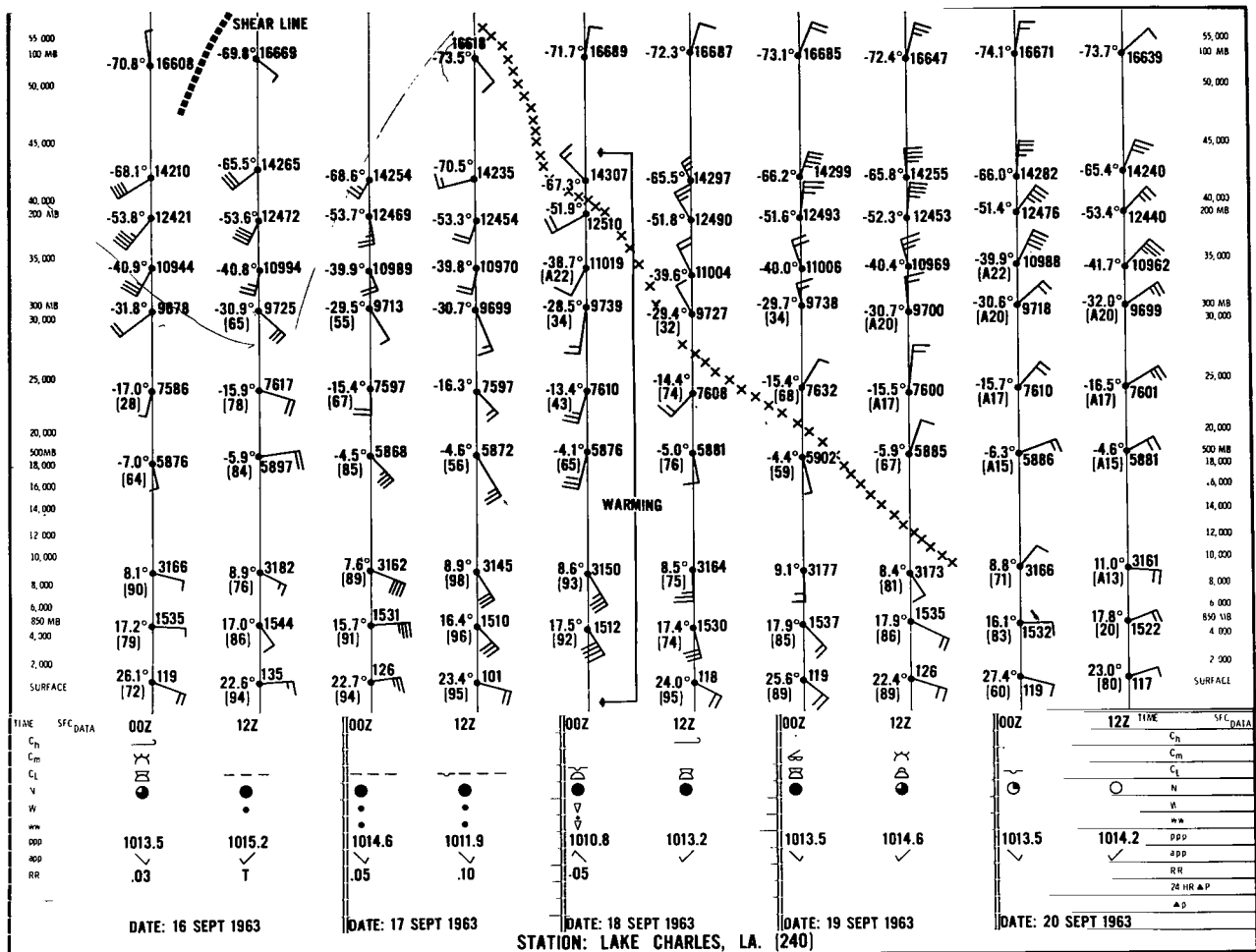


Figure 17-A time cross-section for Lake Charles, Louisiana during the period 16-20 September 1963. The symbol (XXXX) indicates the edge of the ridge line aloft as Hurricane Cindy moved over Lake Charles. The passage of an upper level shear line (—) is indicated on 16 September 1963.

Hurricane Debra

The first appearance of the disturbed area in the southern mid-Atlantic Ocean which was the early tropical depression stage of Debra, was recorded by Tiros VII in an interesting series of television pictures, as shown in Figures 18 and 19. These television pictures were taken at 1300 Z on 17 September and at 1205 Z on 19 September. Concurrent infrared radiation data were recorded during the latter orbit which was analyzed in Figure 20.

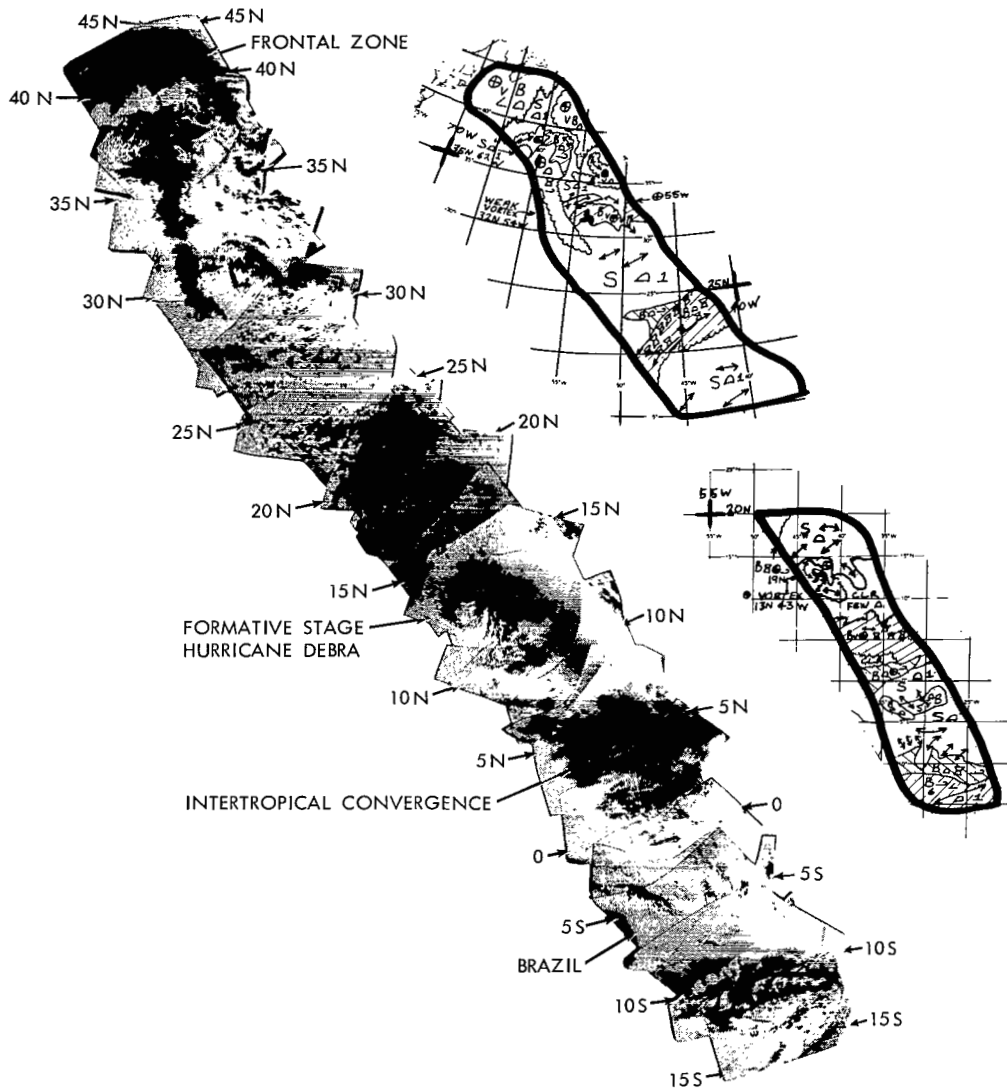


Figure 18—Mosaic and nephanalysis of Tiros VII television pictures indicating Tropical Depression Debra, 1300 Z, 17 September 1963, orbit 1332 (readout 1333 accuracy $\pm 2^\circ$).

The distinctive comma-shaped cloud shown in the two television mosaics is well-defined in the radiation analysis. However the T_{BB} values of 235 to 250°K indicate weak vertical cloud development. The partly cloudy ocean area to the northwest was confirmed by the (275 to 280°K) T_{BB} values.

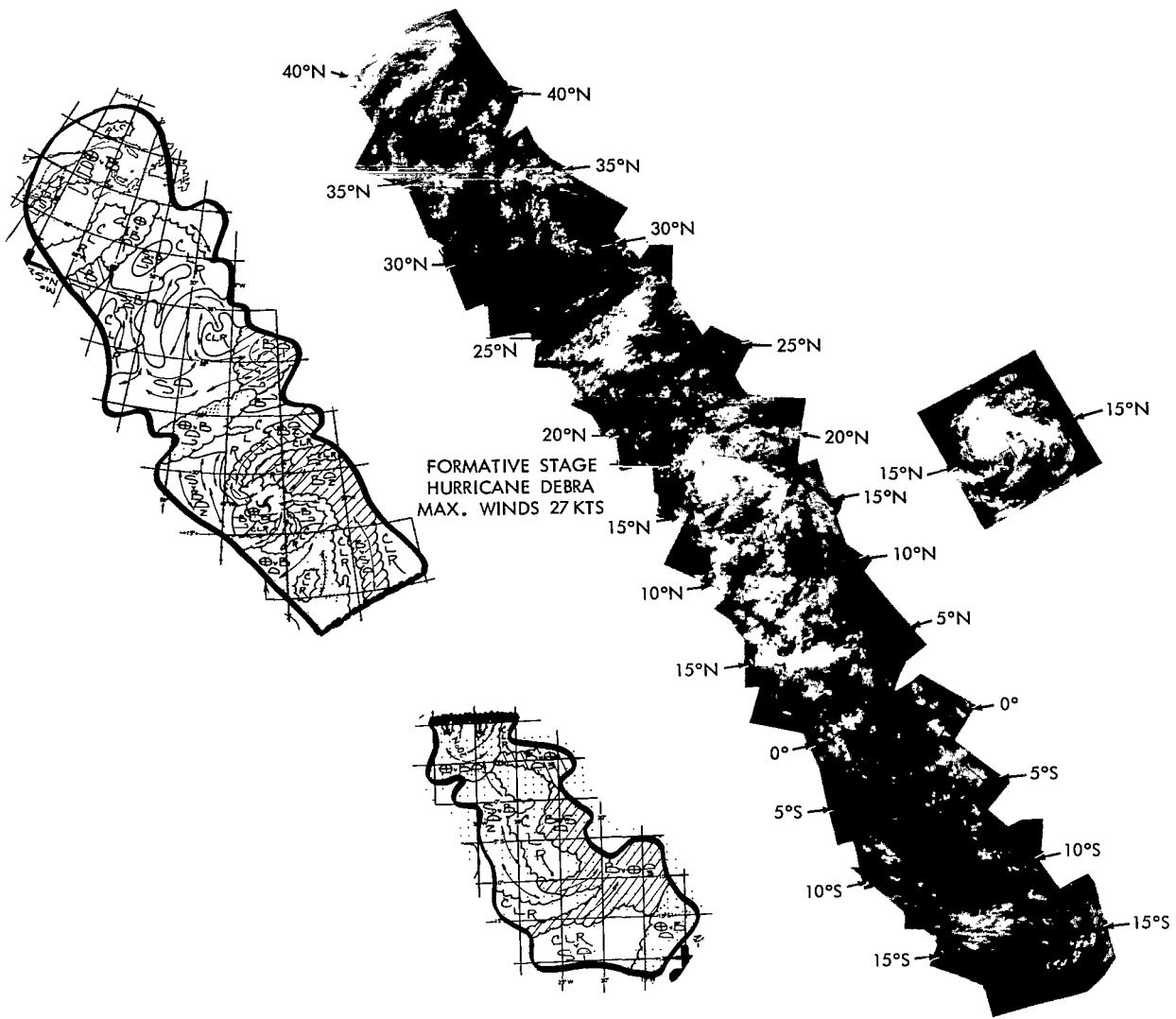


Figure 19-Mosaic and nephanalysis of Tiros VII television pictures indicating Tropical Depression Debra, 1205 Z, 19 September 1963, orbit 1361 (readout 1362 accuracy $\pm 2^\circ$).

Ship reports confirmed the early stage of vortex formation on 19 September and aerial reconnaissance aircraft located a developing eye near 19.3°N , 47.2°W with westerly 25 knot surface winds at 1420 Z on 20 September. On 21 September, at 1654 Z, Debra was named a hurricane when aircraft reported 65 knot surface winds and a minimum central surface pressure of 1000 mb.

Debra remained small in size with a minimal hurricane force for 24 hours as it moved northward on 21-22 September. The storm began to weaken on 23 September 1963 and was finally absorbed into a large extratropical cyclone in the North Atlantic.

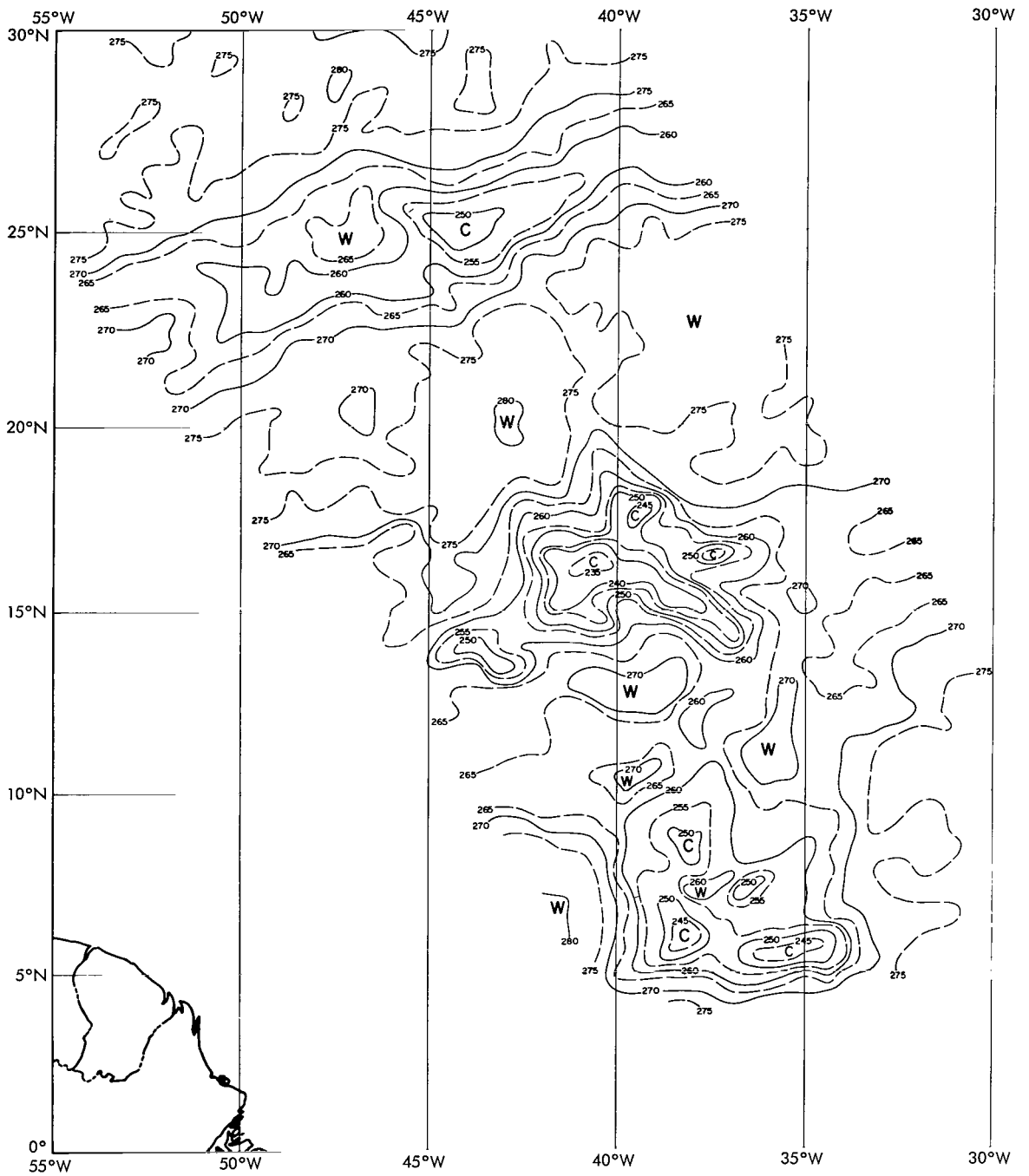


Figure 20—Channel 2 radiation analysis indicating Tropical Depression Debra, 1202–1211 Z, 19 September 1963, orbit 1362. The isolines show T_{BB} values in $^{\circ}K$ (uncorrected for instrumental degradation).

Hurricane Edith

The discovery of Edith in its formative stage can be attributed primarily to Tiros VII television pictures taken over the storm of 23 September 1963. Continuous aerial reconnaissance flights penetrated and tracked the storm from its tropical depression stage to full hurricane stage (127 mps) winds on 25 September) to its final dissipation on 29 September.

A time section (Figure 21) was drawn for San Juan, Puerto Rico, from 22-29 September in order to study the synoptic developments aloft as Hurricane Edith approached and finally passed the station, in the first stages of dissipation. The southerly winds over San Juan from the 500 to 200 mb level is evidence that a high level trough persisted over the Hispaniola area from 22-23 September. A weak easterly wave passed San Juan on 24 September, accompanied by westerly winds in the northern sector of its related anticyclone aloft at the 200 to 300 mb level. Hurricane Edith had entered the Caribbean on 25 September and maximum surface winds of 110 knots were reported. The storm's upper level shear line passage and outflow pattern is shown over San Juan at 0000 to 1200 Z on 26 September. The winds at the 200 to 300 mb level shifted markedly from WNW, 10 to 20 knots to SE-SW and 25 to 45 knots at this time. The presence of the warm core of the hurricane is evident over San Juan at 0000 Z on 27 September.

Tiros VII radiation data was recorded over Hurricane Edith at 0114 Z on 27 September (Figure 22), when the storm was centered approximately over Puerto Rico. The comma-shaped storm and open-wave clouds to the north are shown clearly in the analysis. The cold (225 to 240°K) T_{BB} values relate to the effective radiation cloud heights respectively of 12.1 to 10.5 km (0.2 km lower when corrected for degradation). Aerial reconnaissance at 1130 Z reported cloud tops averaging 35,000 ft (10.6 km) with maxima to 42,000 ft (12.8 km). The eye of the storm was located at 18° 51' N, 69° 20' W at 1226 Z on 27 September. The cloud tops reported by aircraft compares well with the Tiros effective radiation heights even though there was a 9-hour time differential during which the surface winds slowly decreased from 70 to 55 knots.

Figure 23(a) shows a composite of APS-20E radar echoes recorded by reconnaissance aircraft at 1150 to 1258 Z over Edith on 27 September. Figure 23(b) shows the Tiros VII radiation data over Edith at 1137 Z. It should be noted that the moderate to strong radar returns occurred in the southeast and northeast quadrants of the storm which related to the lines of heavy showers in the regions of (220 to 225°K) T_{BB} isotherms. Excellent aircraft cloud photographs and weather reports were made by Mr. Edward J. Zipser, Florida State University, during this fortunate aircraft penetration of Edith in its tropical storm stage. Figure 23(c) describes the cloud types encountered along the aircraft track at 1000 ft between 1100 to 1400 Z on 27 September and Figure 23(d) is a photograph of the N/S line of CB's and heavy showers at 18°N, 68°W at 1150 Z approximately. This line of CB's shows up well as a major radar band in Figure 23(a). Figure 23(e) shows the edge of a CB line with heavy showers and high cirrus anvil clouds at 20.3°N, 70.5°W at 1359 Z approximately.

There appears to be a good correlation between the Tiros radiation data, aircraft cloud photographs and radar reports north and southwest of Puerto Rico, NE and S of Hispaniola.

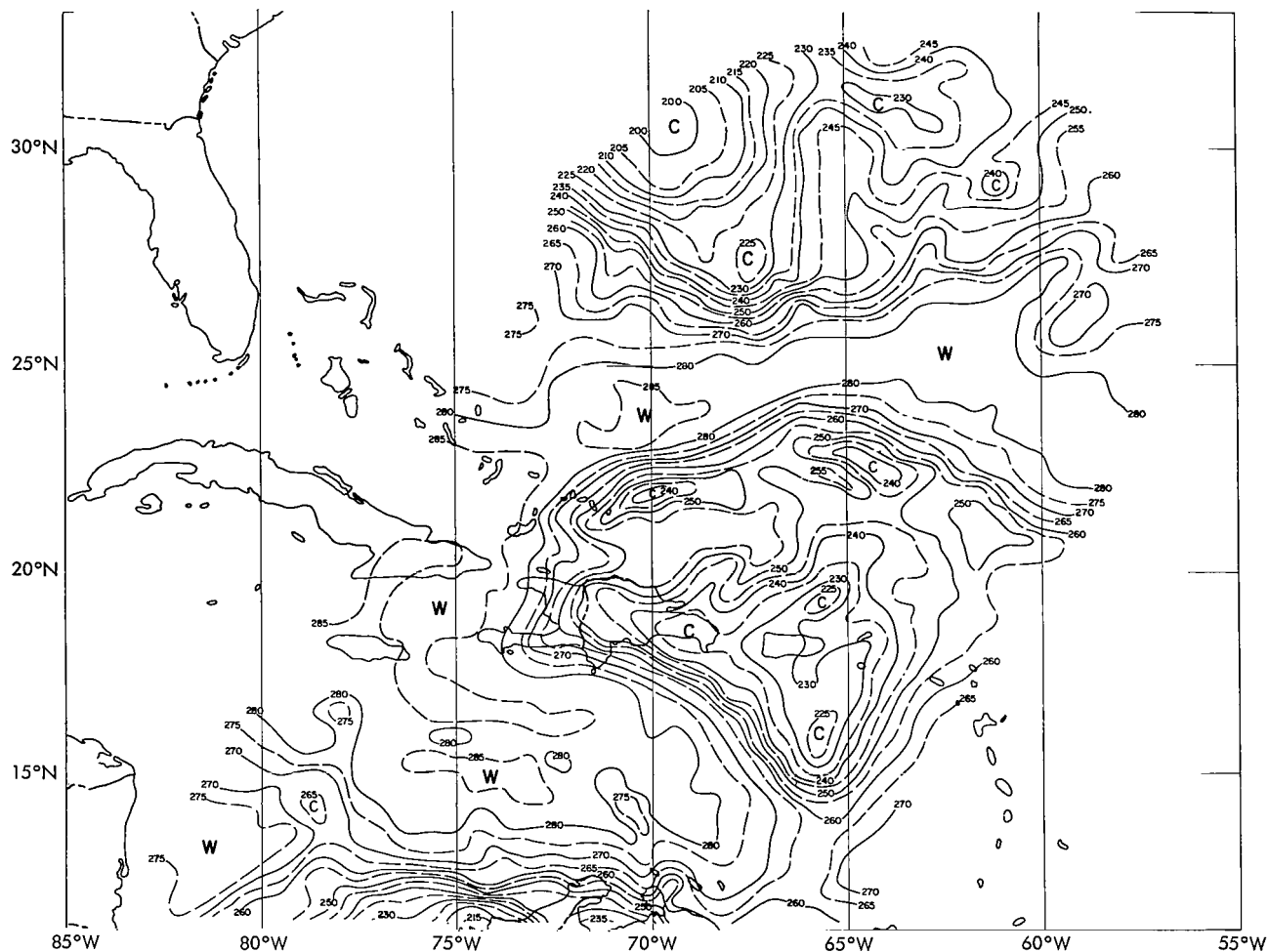
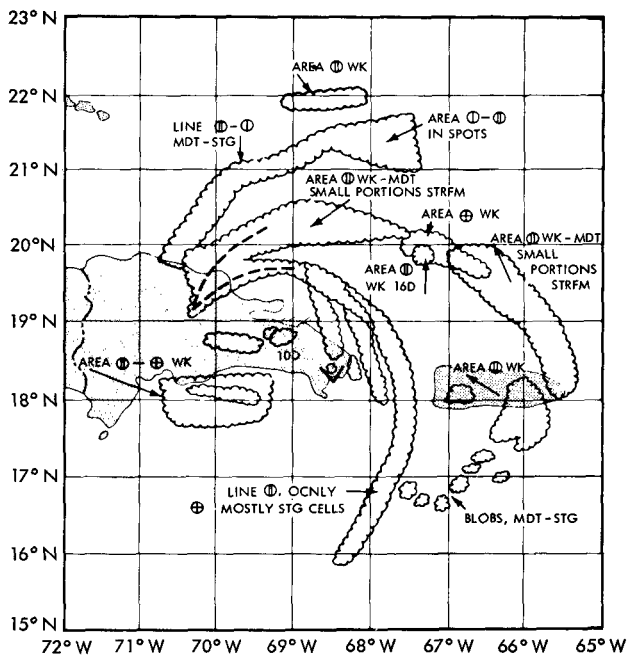
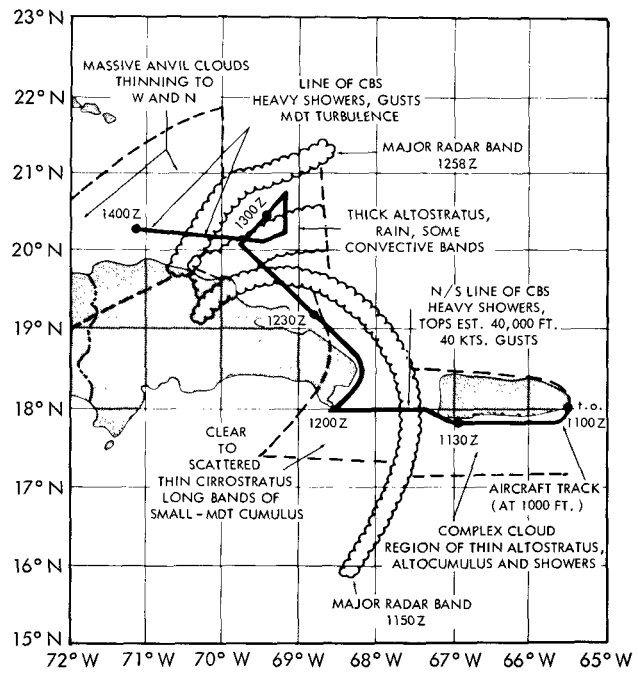


Figure 22—Channel 2 radiation analysis indicating Hurricane Edith, 0114-0122 Z, 27 September 1963, orbit 1473. The isolines show T_{BB} values in $^{\circ}\text{K}$ (uncorrected for instrumental degradation).

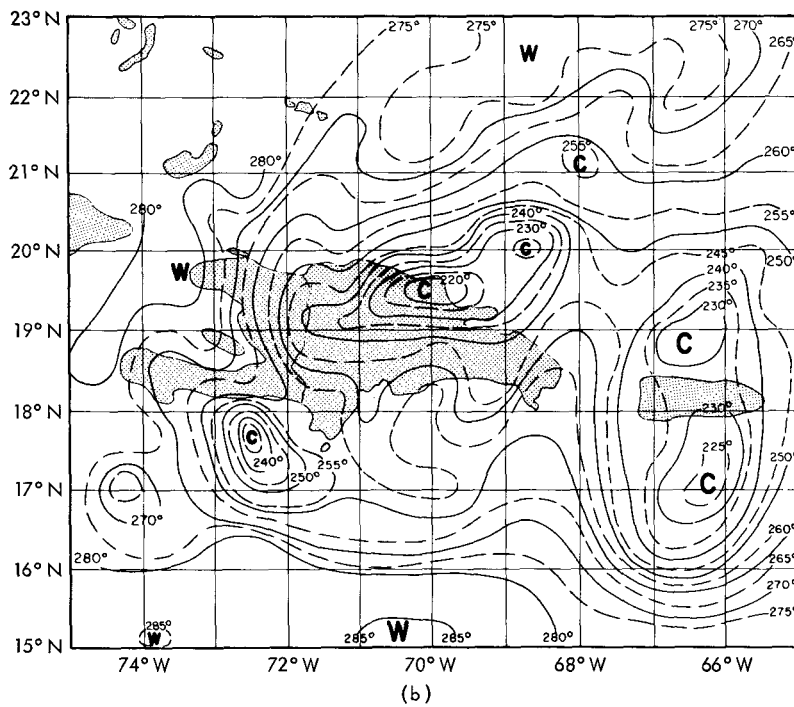
However, since no radar echoes were received over Hispaniola from 71 to 72°W , 19 to 20°N , it is presumed that the clouds, as shown by the radiation data, contained little precipitation and hence were essentially transparent to the 10 cm radar energy. Television pictures of Edith (Figure 24) taken by Tiros VI at 1243 Z, 27 September were recorded within one hour approximately of the San Juan radiosonde ascent (Figure 21), aircraft reconnaissance reports and Tiros VII radiation data. Besides confirming the general outlines of the storm, three particular cloud details show good correspondence when comparing Figures 23(b) and 24: (a) A clear wedge in the storm's cloud canopy at 19°N , 73°W , (b) An isolated cloud mass in the SW quadrant of the storm at 17.5°N , 72.5°W , (c) A cloud mass at 21°N , 68°W .



(a)



(c)

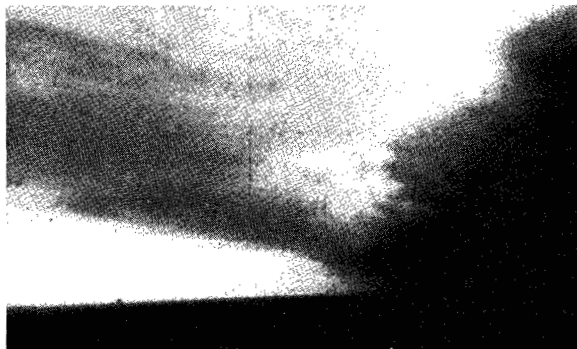


(b)

Figure 23-(a) Composite of U.S. Navy reconnaissance aircraft APS-20E (10 cm) radar echoes from Hurricane Edith, 1150-1258 Z, 27 September 1963; (b) Channel 2 radiation analysis indicating Hurricane Edith, 1137-1140 Z, 27 September 1963, orbit 1480. The isolines show T_{BB} values in $^{\circ}K$ (uncorrected for instrumental degradation); (c) Composite of U.S. Navy reconnaissance aircraft APS-20E radar echoes from Hurricane Edith, (partial coverage) 1150-1258 Z, 27 September 1963 and aircraft reconnaissance weather echoes reports, during the penetration of Hurricane Edith, 1100-1400 Z, 27 September 1963.



(d)



(e)

Figure 23—(d) Aircraft photograph of a N/S line of CB cells and heavy showers in Hurricane Edith at 18°N, 68°W at 1150 Z approximately, 27 September 1963; (e) Aircraft photograph of the edge of a CB line with heavy showers and high cirrus anvil clouds in Hurricane Edith at 20.3°N, 70.5°W at 1359 Z approximately, 27 September 1963.

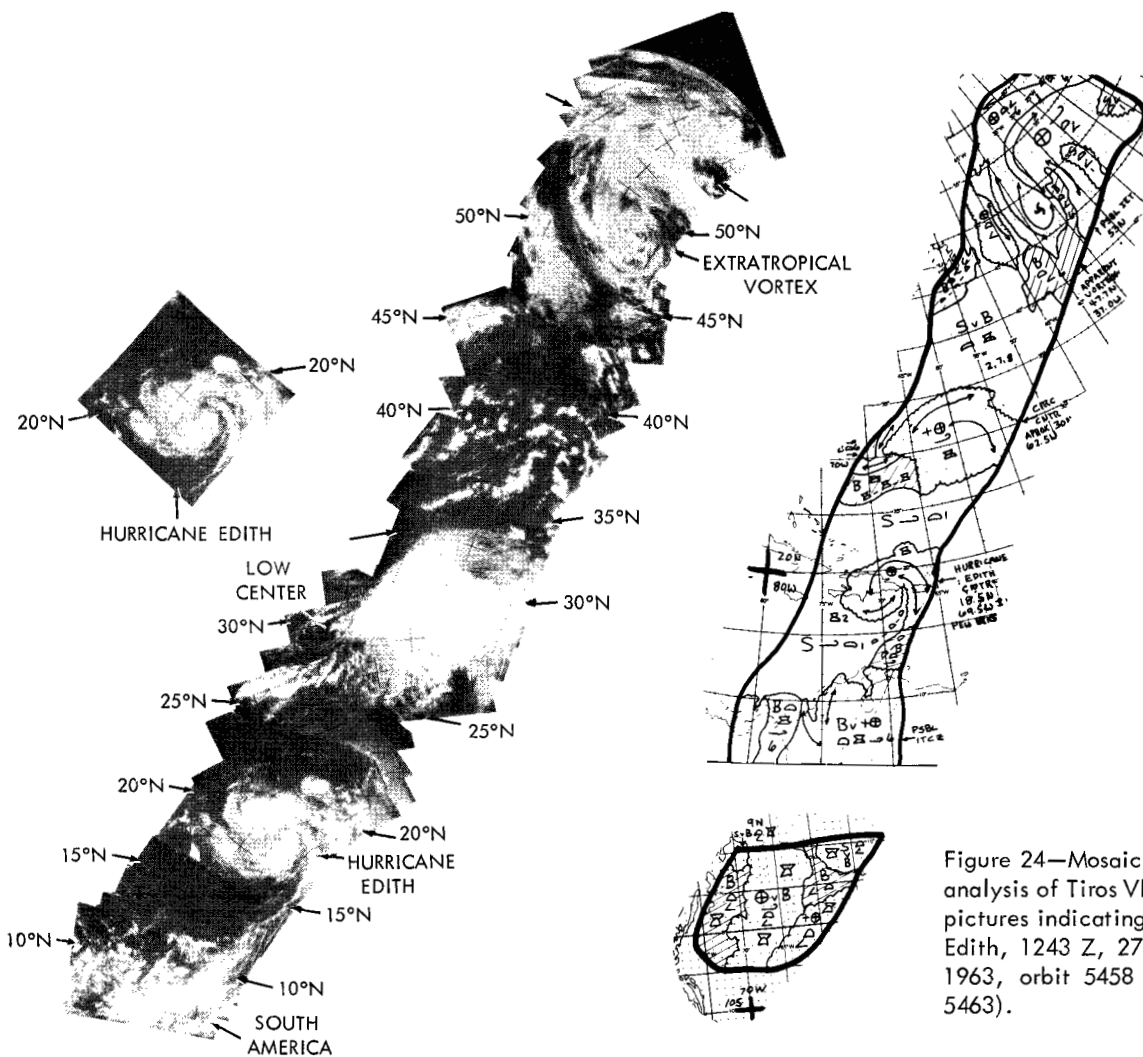


Figure 24—Mosaic and neph-analysis of Tiros VI television pictures indicating Hurricane Edith, 1243 Z, 27 September 1963, orbit 5458 (readout 5463).

Edith moved slowly northwestward on 27 September after having been weakened by the mountains and hills of Hispaniola and Puerto Rico. A frontal wave at 30°N, 69°W moving NE ahead of Edith (Figure 25), had weakened the surface pressure gradient over the S. Bahamas, thus weakening the low level flow north of the storm and the upper inverted trough had flattened in a generally easterly flow.

The final hours of the dissipation of Edith are depicted in a Tiros VI television picture and nephanalysis at 1229 Z, 29 September as shown in Figure 26. The cloud canopy diameter had decreased from 8° on 27 September (Figure 24) to approximately 4.5° on 29 September (Figure 26), with the attendant decay of storm's cloud structure. Reports of scattered squalls with 25 knot surface winds were all that remained of the once violent Caribbean storm on 29 September 1963.

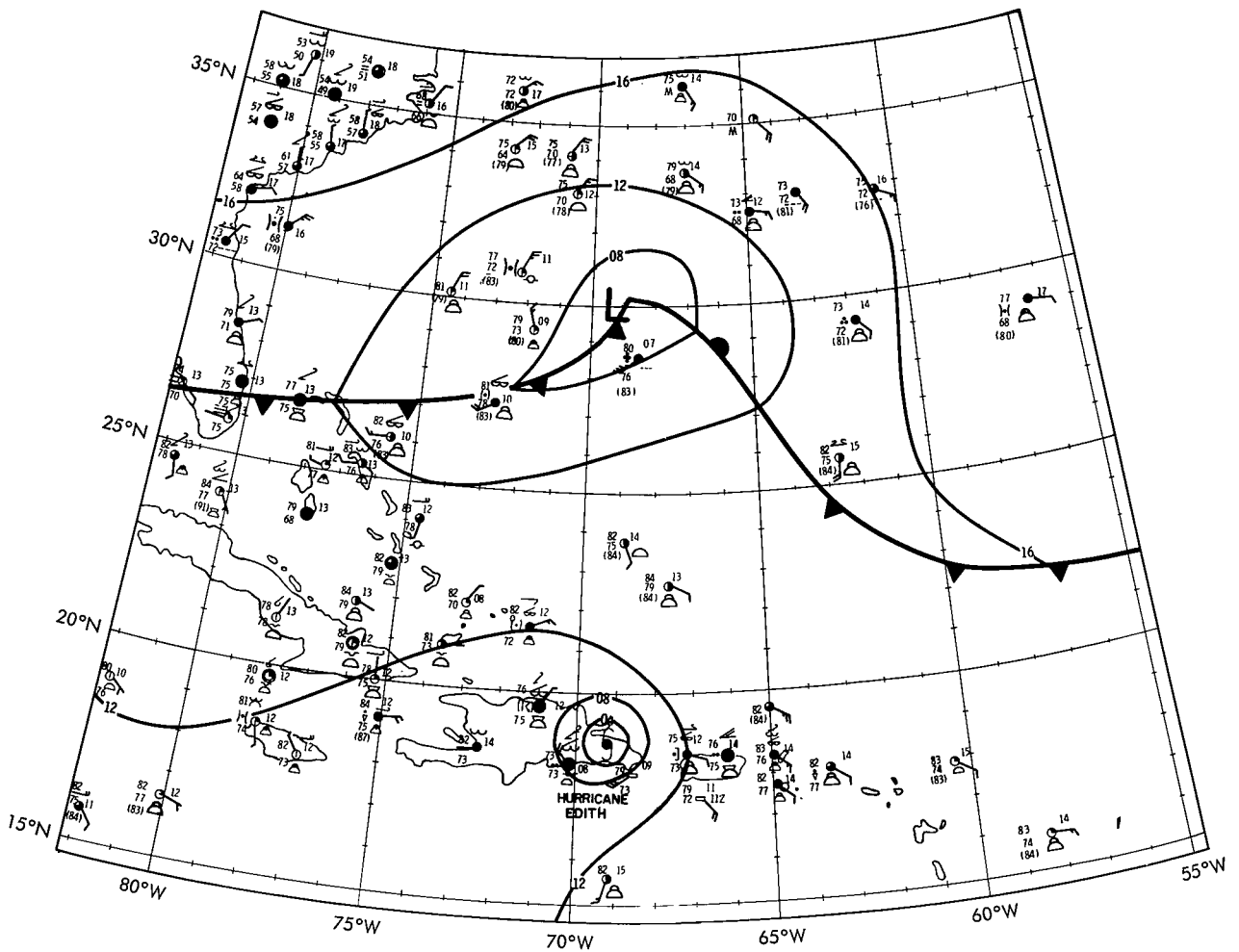


Figure 25-Surface synoptic chart, 1200 Z, 27 September 1963, indicating Hurricane Edith (National Meteorological Center, U.S. Weather Bureau).

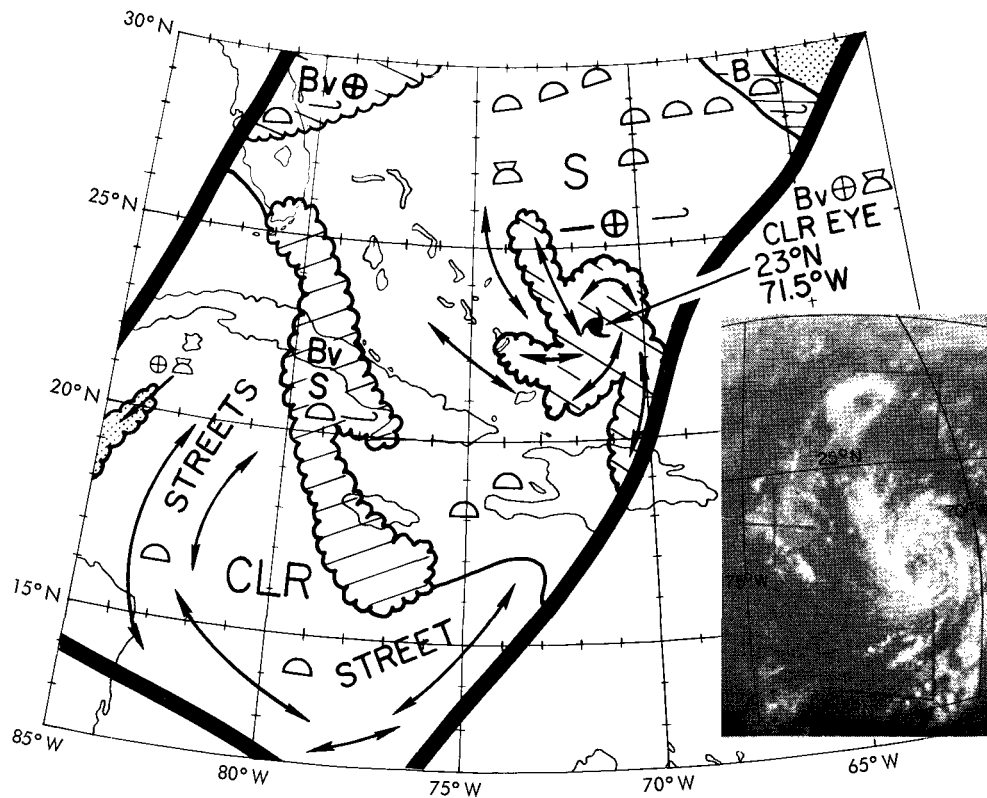


Figure 26-Nephanalysis and Tiros VI television picture indicating the dissipative stage of Hurricane Edith, 1229 Z, 29 September 1963, orbit 5491.

Hurricane Flora

Hurricane Flora was one of the most destructive hurricanes in the recent history of Cuba and Haiti. More than 7000 persons lost their lives and disastrous property damage amounting to over \$500,000,000 during the period 3-9 October 1963 was reported.

Flora was detected by Tiros VII on 26-27 September in the southern North Atlantic and was tracked by aerial reconnaissance on 30 September after it reached the hurricane stage. The storm increased in size and intensity after it entered the Caribbean on 1 October, soon becoming "the best organized tropical cyclone to appear in two years" (Reference 6).

Figure 27 is the only available Tiros VII radiation data at 1004 Z on 2 October recorded over Flora which shows the complete outline of this warm core storm. The cold (205 to 210°K) T_{BB} values relate to the effective radiation cloud heights respectively of 14 to 13.5 km (0.1 km lower when corrected for degradation). The tropopause was indicated at the 15.5 km level. A large cirroform cloud canopy, outlined by the (220 to 230°K) T_{BB} values (12 to 11 km), indicates a strong anticyclonic outflow aloft. This figure illustrates graphically how the radiation data can describe the cloud-top temperatures, and hence cloud heights over a violent intensifying tropical hurricane (124 kts). It is of interest to note that the Hurricane Flora (Figure 27) and Tropical Disturbance Beulah (Figure 6) have similar cold (210 to 250°K) T_{BB} values. The most significant

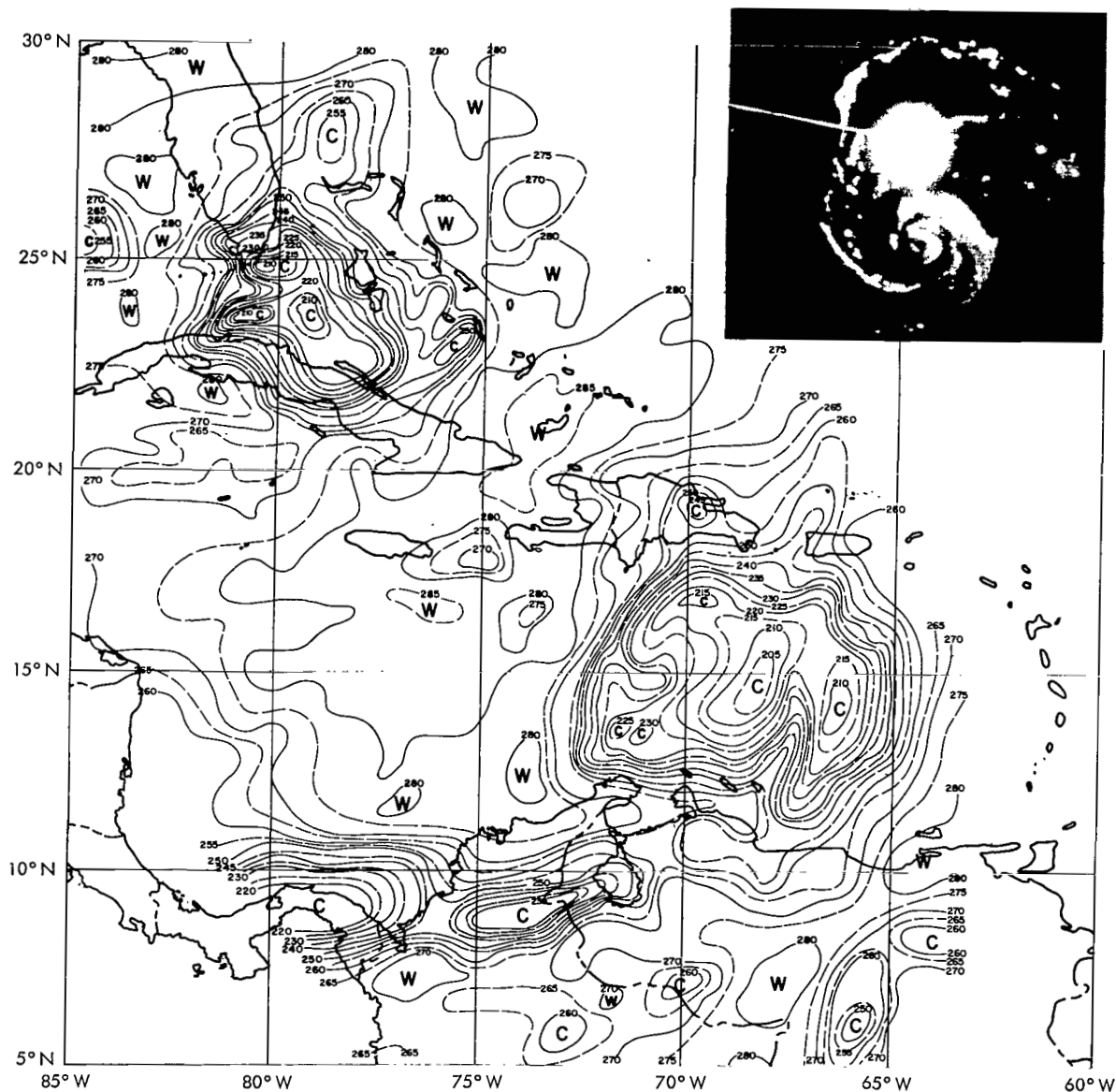


Figure 27—Channel 2 radiation analysis indicating Hurricane Flora, 1004-1012 Z, 2 October 1963, orbit 1553. The isolines show T_{BB} values in $^{\circ}\text{K}$ (uncorrected for instrumental degradation), U.S. Navy reconnaissance aircraft radar photograph indicating Hurricane Flora, 1100 Z approximately, 2 October 1963, 250 mile range.

difference between them is their size and degree of organization. An aircraft radar photograph, showing the eye and spiral bands of Flora at 1100 Z approximately on 2 October, is shown in the inset in Figure 27. The cold (210 to 235 $^{\circ}\text{K}$) T_{BB} values shown over the Florida Straits are indications of a stationary front which was located in that region. Remnants of this front are seen in the surface map in Figure 28. A waterspout was reported at Ft. Lauderdale, Florida at 1800 Z 2 October, which tends to confirm the instability of this cloudy subtropical region.

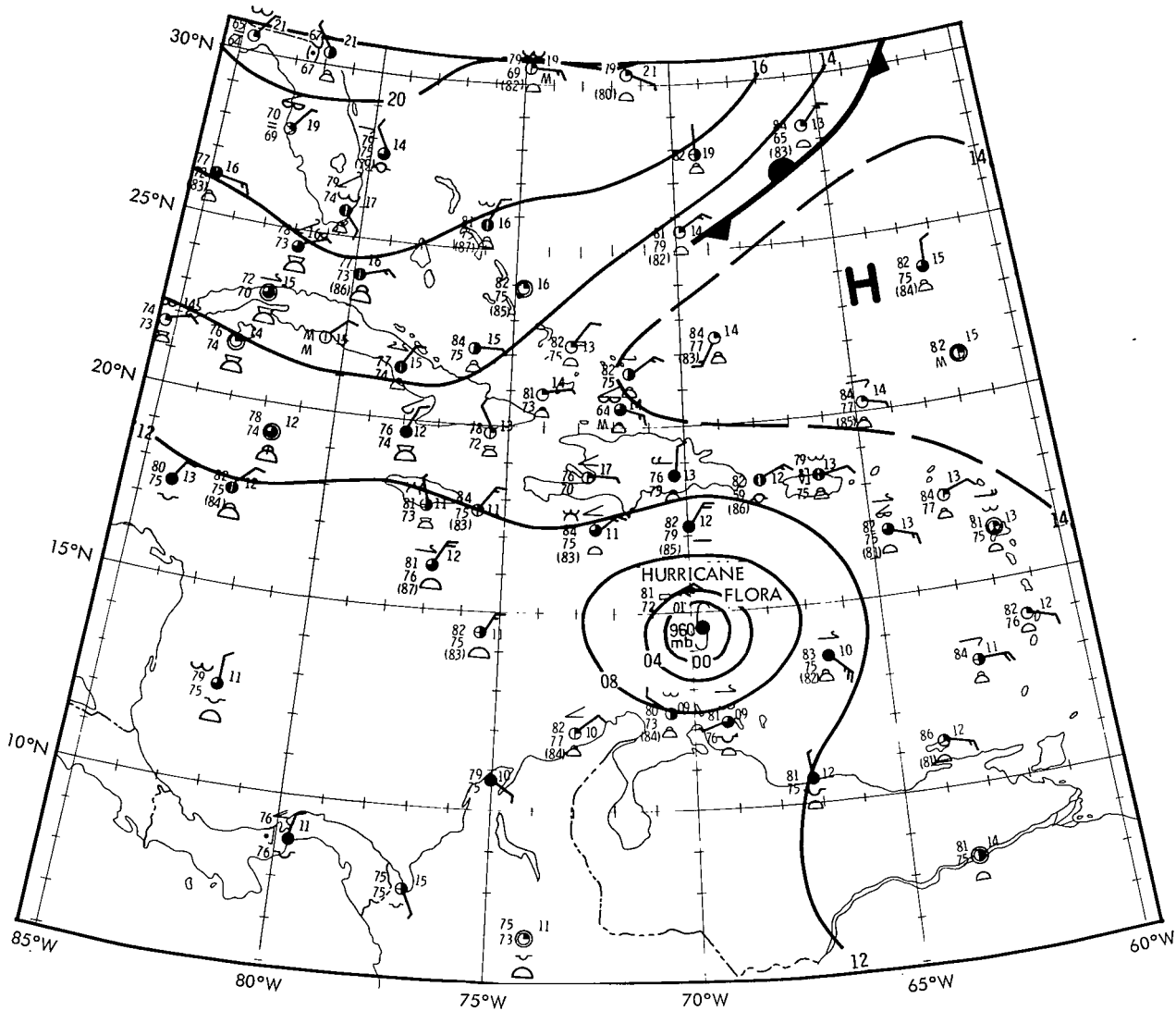


Figure 28—Surface synoptic chart, 1200 Z, 2 October 1963, indicating Hurricane Flora (National Meteorological Center, U.S. Weather Bureau).

At 1342 Z, on 2 October, a well-defined eye, 11 miles in diameter, was detected by aircraft radar. The eye wall was closed in all quadrants; wall clouds were 8 miles (12.8 km) thick with tops above 50,000 ft (15.2 km) where moderate to heavy turbulence was encountered. A maximum observed surface wind of 130 knots and minimum surface low pressure of 968 mb was reported.

From 3-8 October, Flora meandered toward and over eastern Cuba where maximum surface winds of 140 mph (122 kts) with peak gusts of 180 to 200 mph (156 to 174 kts) were reported. Navy reconnaissance reported 10,000 ft (3 km) flight level winds of 145 kts and a minimum central surface pressure of 954 and 936 mb during 2-3 October.

Enormous amounts of rainfall (90 in. near Velasco, Cuba) were recorded over Haiti, Jamaica and Cuba. The erratic and slow movement of the storm from 3-8 October was caused by the

effects of high pressure areas to the west, east and north, which boxed in Flora and blocked movement. The storm started to move to the NE under the influence of a polar trough by 8 October, and finally lost its tropical characteristics in the North Atlantic.

Hurricane Ginny

Hurricane Ginny was unusual because of its meandering double-looped trajectory off the southeast coast of the United States and its relatively light precipitation content. Ginny formed on an easterly wave in the Bahamas on 16 October 1963 as this wave moved under a trough in the westerlies. The storm moved northward and changed from a cold core to a warm core storm on 21 October over the warm waters of the Gulf Stream off of Cape Hatteras. By 22 October, Ginny completed a clockwise loop east of Hatteras and began to accelerate to the southwest. This southerly movement was caused by the effect of a strong ridge moving eastward over New England. The storm decreased to tropical storm intensity by 24 October but it reintensified in the Gulf stream, 90 miles ENE of Cape Kennedy, Florida. Ginny then completed her second clockwise loop and proceeded north with winds reaching 90 knots, on 25 October. Figure 29 shows the erratic cycloidal gyrations of the eye as recorded by WSR-57 radar at Charleston, S.C., from 25-26 October.

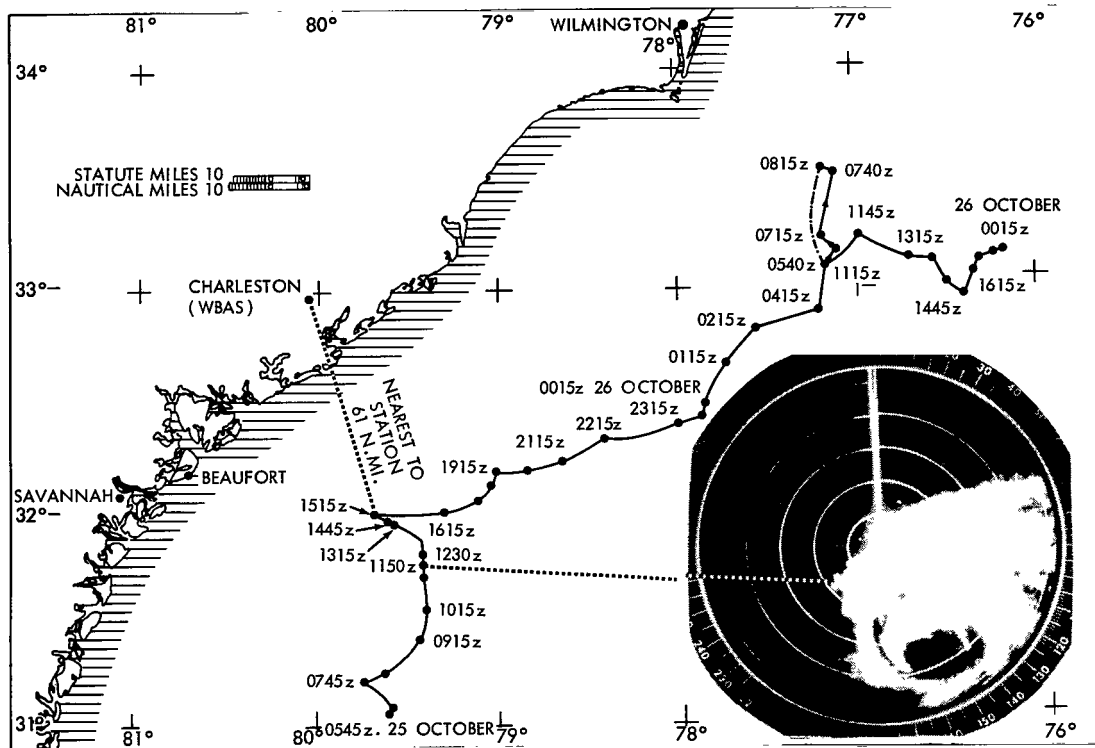


Figure 29—Cycloidal gyrations of path of eye of Hurricane Ginny recorded by WSR-57 radar at WBAS, Charleston, S. C., 0545 Z, 25 October 1963 to 1915 Z, 26 October 1963 (Courtesy U.S. Weather Bureau).

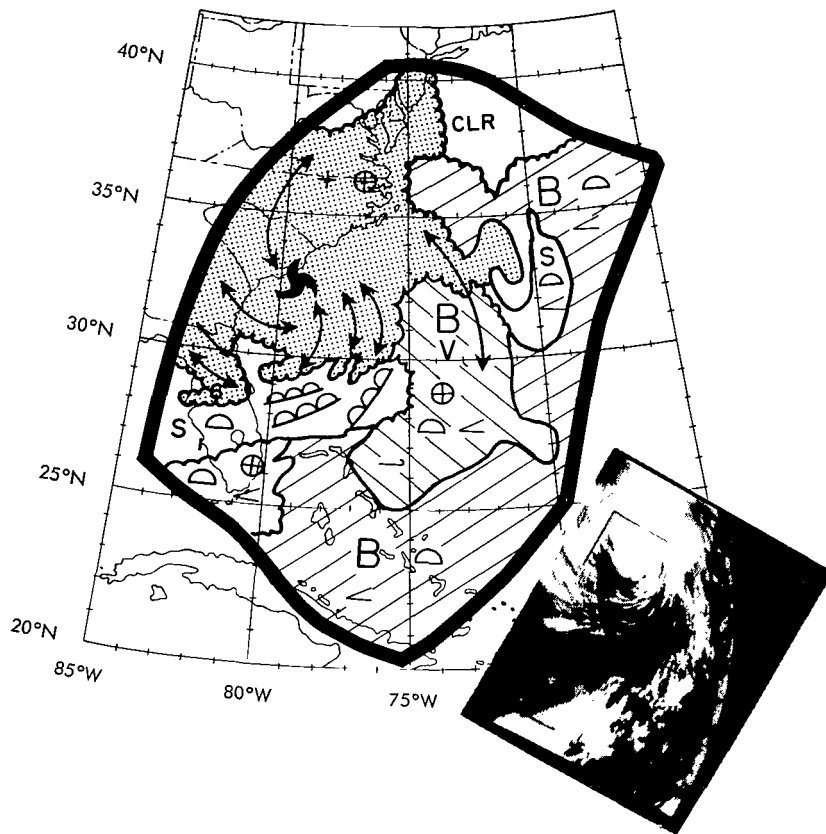


Figure 30-Nephanalysis and Tiros VII television picture Hurricane Ginny, 1741 Z, 25 October 1963, orbit 1897.

Tiros VII television cameras located Ginny on 25 October at 1741 Z off the South Carolina coast. Figure 30 shows a frame from this television sequence and the resulting nephanalysis. The 5-channel radiometer recorded the cloud details of Hurricane Ginny 8-1/2 hours later (0211 Z) at night. The channel 2 radiation analysis from this orbit is shown in Figure 31. The elongated double-centered main cloud canopy with its short tail cloud, extended northeastward to off-shore cloudiness near New England. The (220 to 230°K) T_{BB} values relate to the effective radiation cloud heights respectively of 11.5 to 10.5 km (0.2 km lower when corrected for degradation).

Aerial reconnaissance reported a radar eye 28 miles in diameter, centered at 32° 52'N, 76° 16'W at 0157 Z on 26 October. Wall cloud tops averaged 36,000 ft (10.9 km) with maxima to above 40,000 ft (12.2 km). These cloud heights compare favorably (± 1 km) with the Tiros effective radiation cloud tops. Minimum central surface pressure and maximum surface winds were 979 mb and 84 kts respectively. The surface weather chart for 0300 Z on 26 October, shown in Figure 32, compares well with Figure 31 for the hurricane's position and areas of cloudiness.

The next television coverage over Ginny which confirmed the storm features described above was made at 1806 Z on 26 October. A frame of this sequence is shown in Figure 33. Nearly 24 hours later during the daytime at 1645 Z, simultaneous television and radiation coverage of

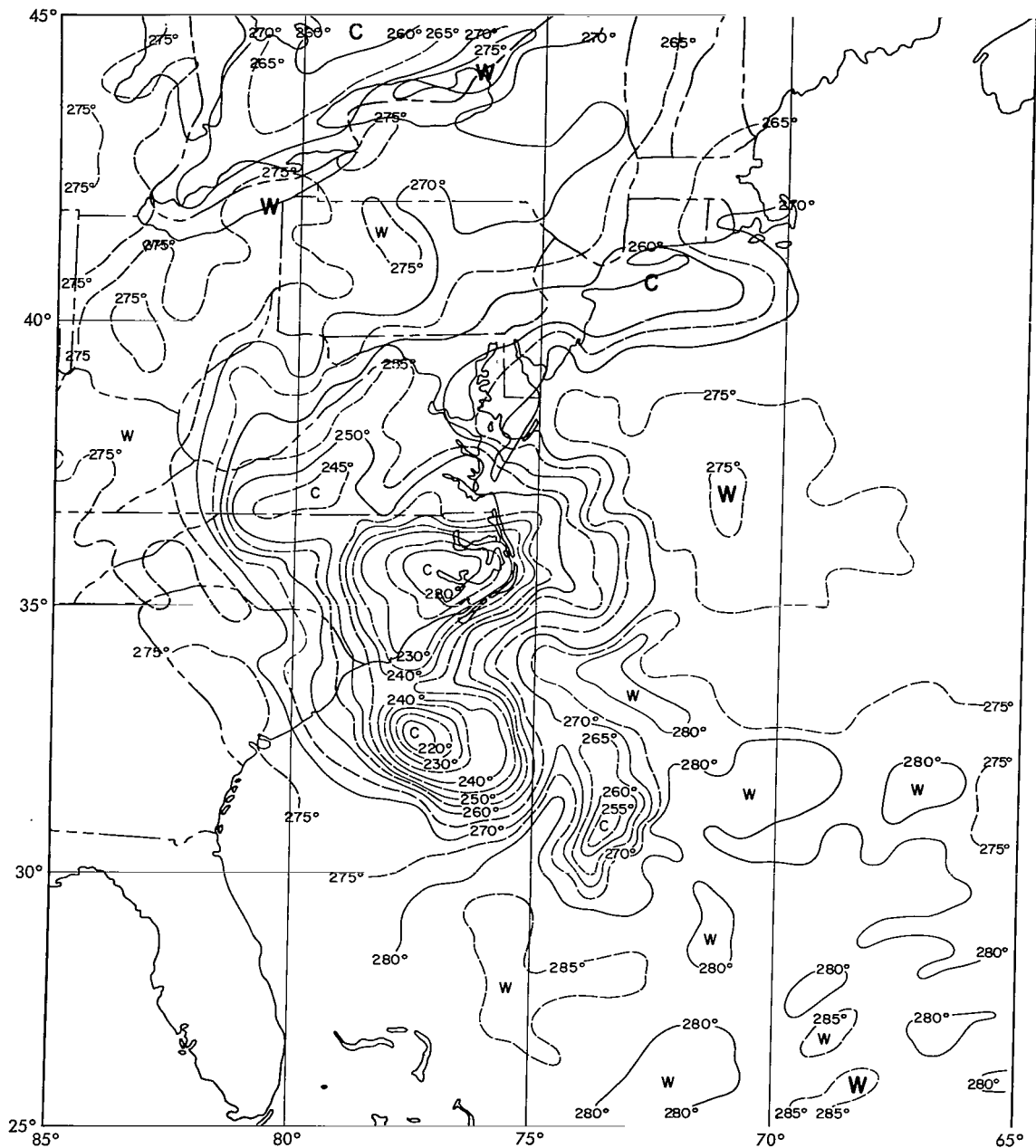


Figure 31—Channel 2 radiation analysis indicating Hurricane Ginny, 0211-0217 Z, 26 October 1963, orbit 1903. The isolines show T_{BB} values in $^{\circ}K$ (uncorrected for instrumental degradation).

Ginny was obtained and are shown in Figures 34 and 35. The eye appears visible at $32.5^{\circ}N$, $75^{\circ}W$ approximately in Figure 34 which places it under the slightly warmer $235^{\circ}K$ T_{BB} isotherm. The thin cirrus clouds seen in the television insert were not detected by the Tiros radiometer for several reasons. First, these clouds appear to lack sufficient depth or opacity to emit as a uniform radiating surface or blackbody and secondly, the clouds measure only 15 nautical miles (28 km) in their cross-dimension. The minimum diameter of the radiometer scan spot is 35 nautical miles (65 km) which is too coarse in resolution to detect the narrow cirrus streamers.

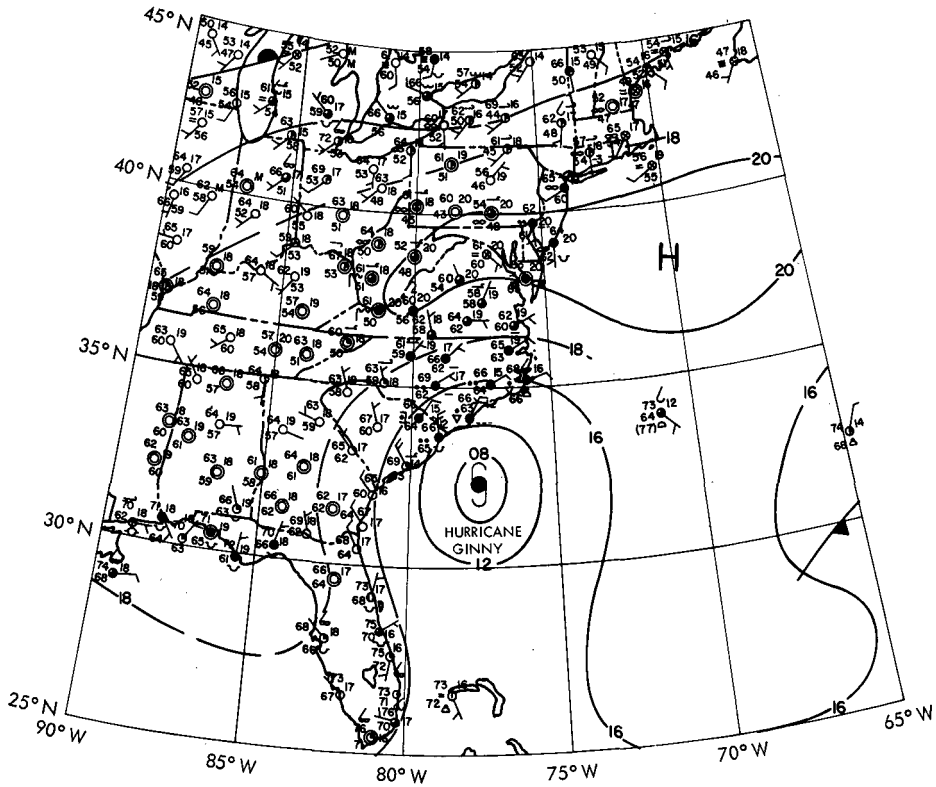


Figure 32—Surface synoptic chart, 0300 Z, 26 October 1963, indicating Hurricane Ginny (National Meteorological Center, U.S. Weather Bureau).

A final radiation chart over Ginny was drawn at 0119 Z on 28 October as shown in Figure 36. The main body of the storm had moved eastward with a slight increase in intensity. A pronounced tail cloud is shown extending to the south while the cloudiness of the NE coast still persists as previously shown in Figure 31. The cool (245 to 260°K) T_{BB} values oriented NE/SW across Pennsylvania and New York State relate to the cold frontal cloudiness shown on the 0300 Z surface chart in Figure 37 on the same date. Figure 38 shows the typical warm anticyclonic outflow pattern at the 300 mb level for a storm of this intensity. A strong polar jet is seen to the north of Ginny while a weaker subtropical jet curves to the SE away from the storm.

An interesting warming region is shown in Figure 39 which occurred aloft (11 to 14 km

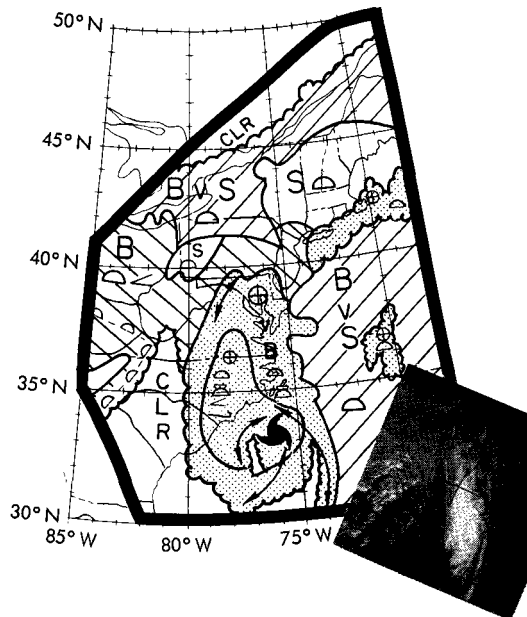


Figure 33—Nephanalysis and Tiros VII television picture indicating Hurricane Ginny, 1806 Z, 26 October 1963, orbit 1912.

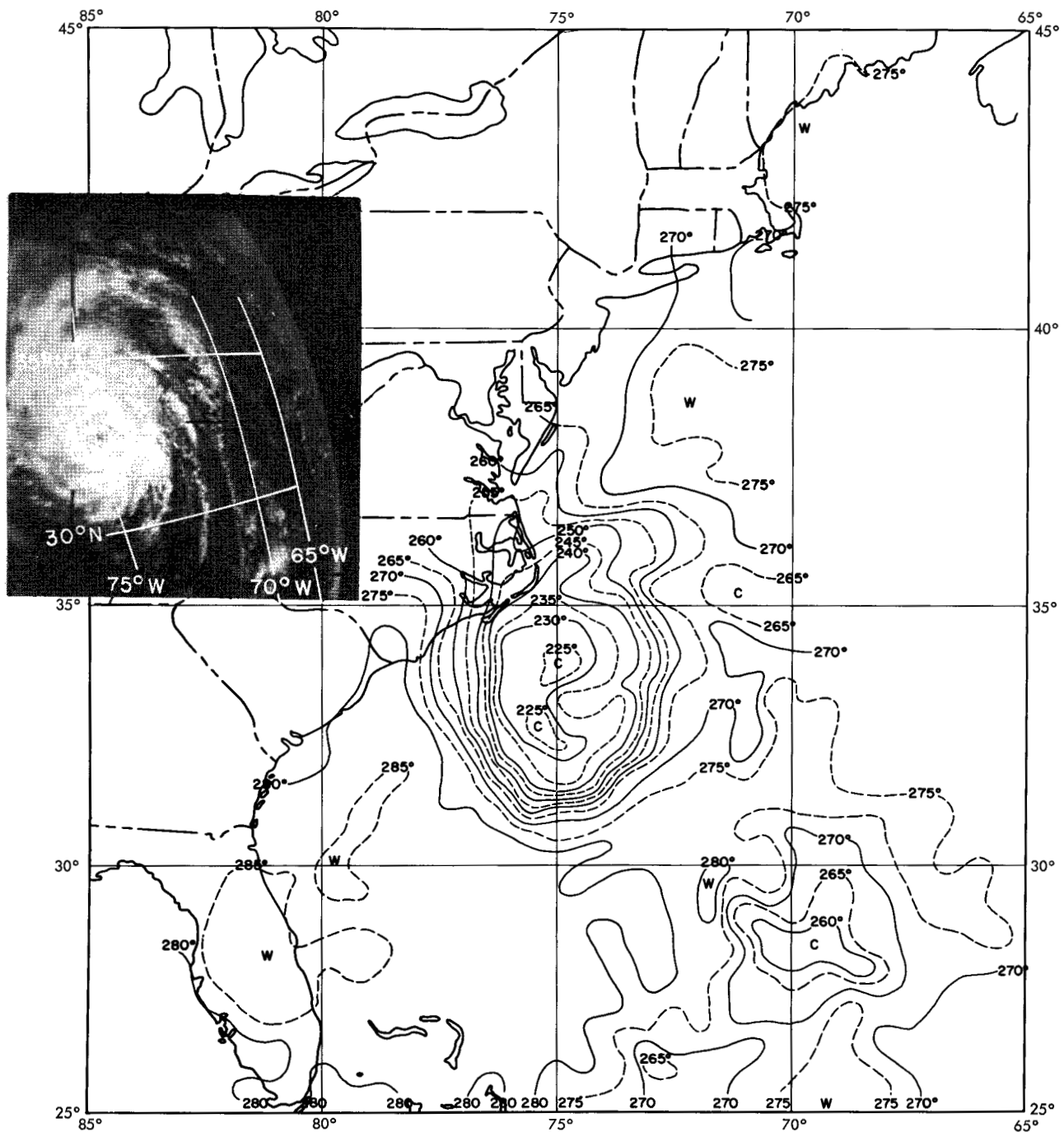


Figure 34—Channel 2 radiation analysis indicating Hurricane Ginny, 1645–1649 Z, 27 October 1963, orbit 1926. The isolines show T_{BB} values in $^{\circ}\text{K}$ (uncorrected for instrumental degradation), Tيروس VII television picture of Hurricane Ginny, 1646 Z, 27 October 1963.

approximately) over Charleston, Norfolk, Washington, D.C., and Greensboro during the 3 day period, 25–28 October, when Hurricane Ginny gradually moved away from the eastern shoreline. This warming could be explained by warm air advection and/or subsidence along the outer perimeter of the hurricane (Reference 19).

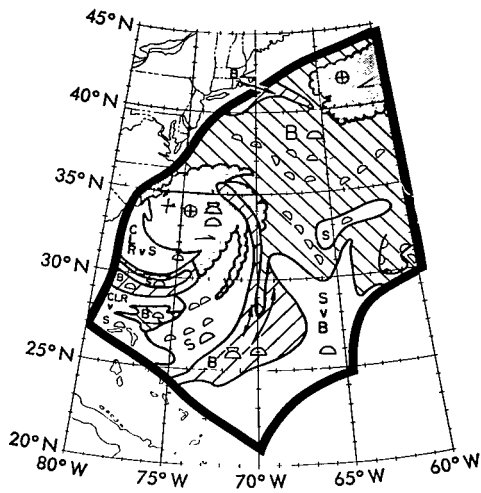
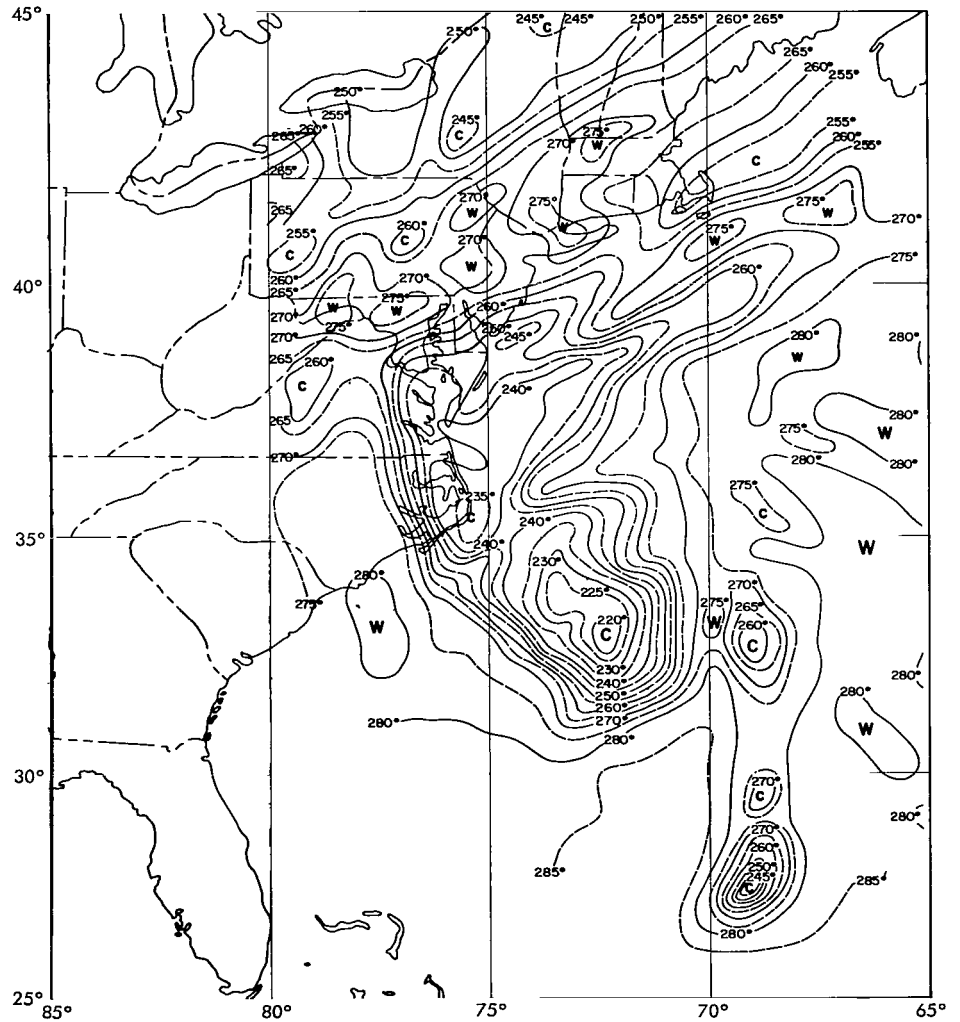


Figure 35—Nephanalysis of Tiros VII television pictures indicating Hurricane Ginny, 1646 Z, 27 October 1963, orbit 1926.

Figure 36—Channel 2 radiation analysis indicating Hurricane Ginny, 0119-0125 Z, 28 October 1963, orbit 1932. The isolines show T_{BB} values in $^{\circ}K$ (uncorrected for instrumental degradation).



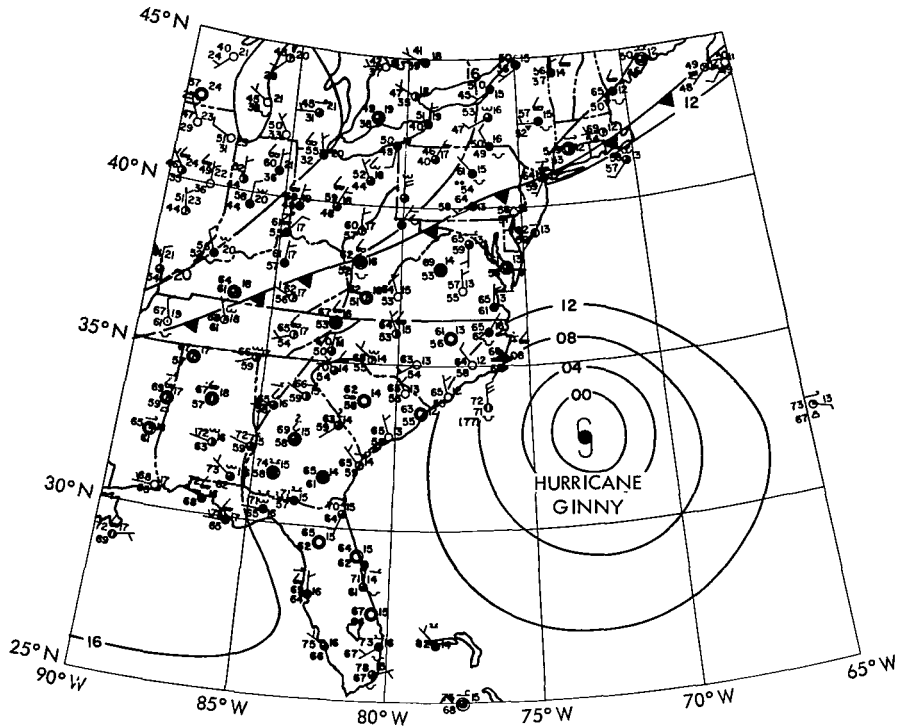


Figure 37—Surface synoptic chart, 0300 Z, 28 October 1963, indicating Hurricane Ginny (National Meteorological Center, U.S. Weather Bureau).

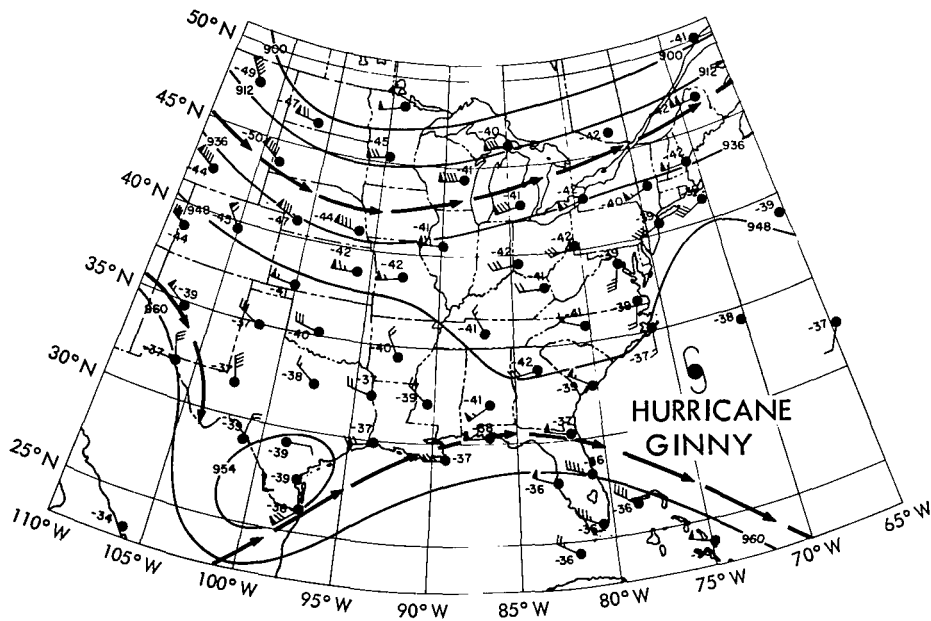


Figure 38—300 mb Constant Pressure Chart, 000 Z, 28 October 1963, indicating Hurricane Ginny (National Meteorological Center, U.S. Weather Bureau).

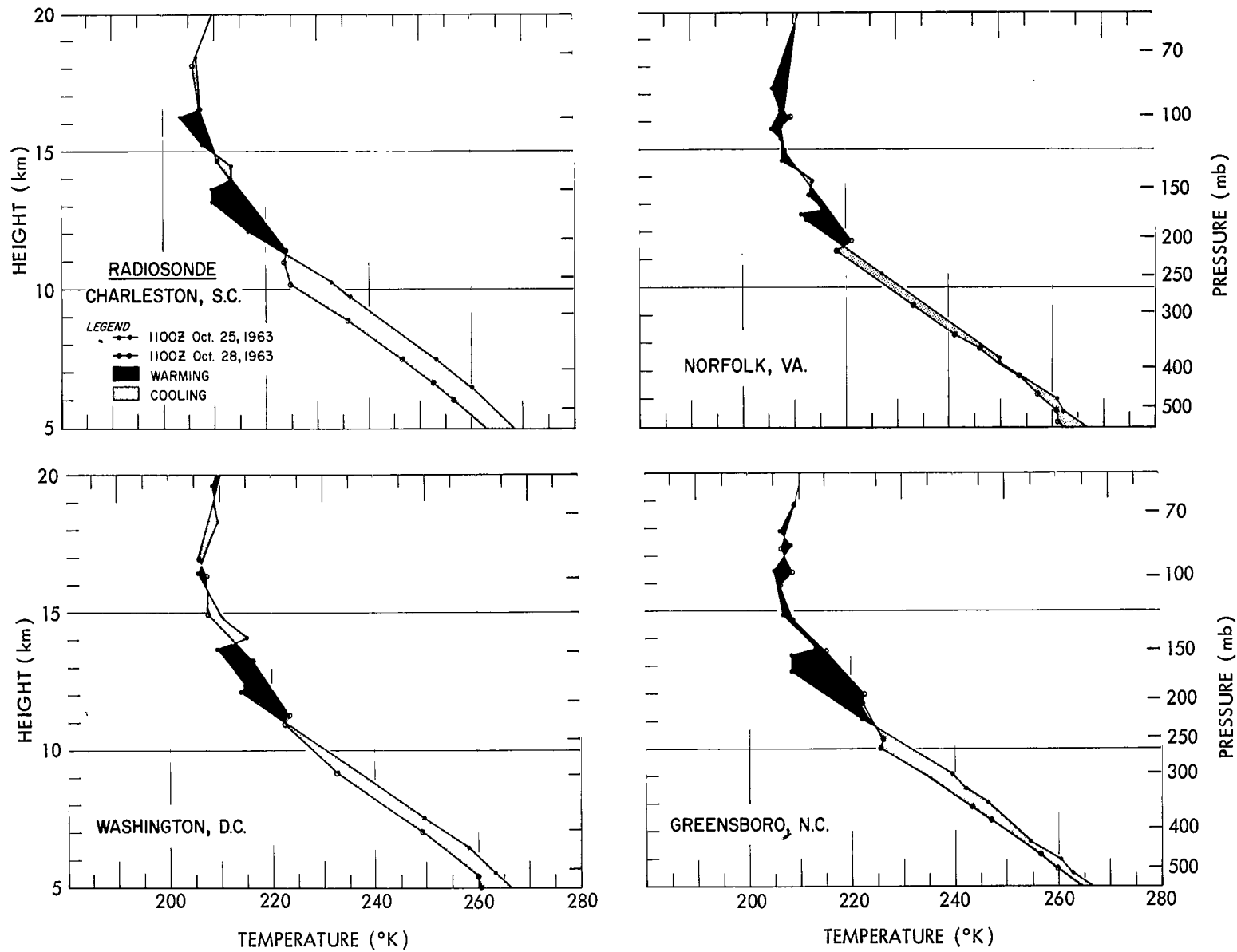


Figure 39-3-Day Upper Air Temperature Change Chart (5-20 km), using radiosonde data for Charleston, S.C., Washington, D.C., Norfolk, Va., Greensboro, N.C., 1100 Z, 25-28 October 1963.

The last of this series of Tiros VII television pictures over Ginny were taken at 1709 Z on 28 October. One of these pictures is shown in Figure 40. The storm is increasing again in intensity and the eye is located at 34.7°N, 71.8°W approximately. By 29 October 1963, Ginny had moved NE towards Nova Scotia and became extratropical in its characteristics.

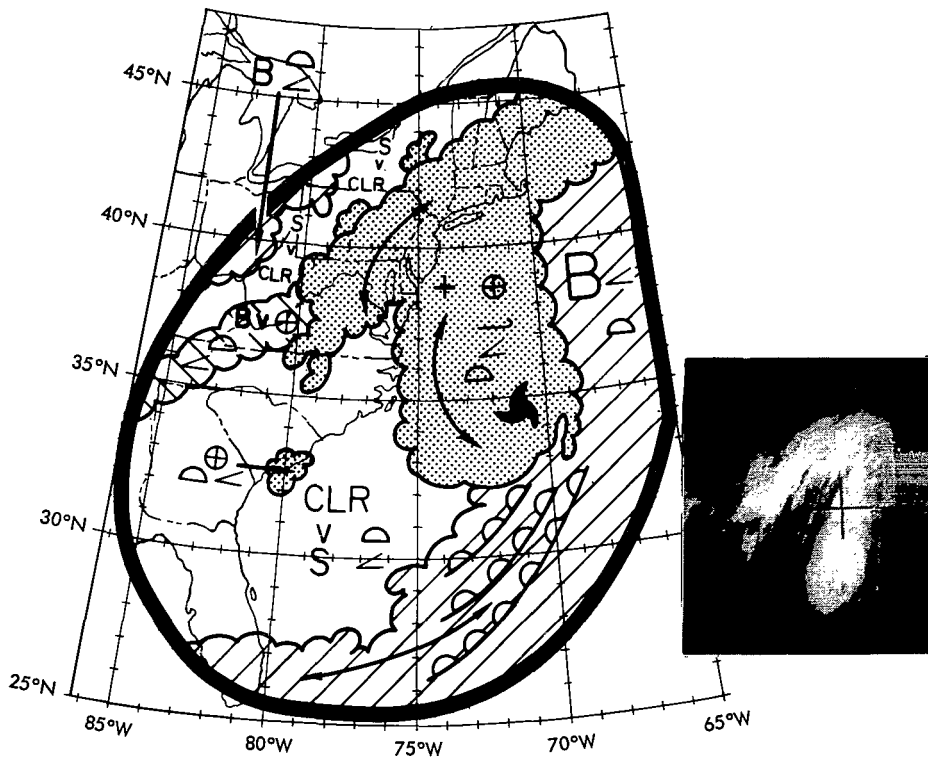


Figure 40—Nephanalysis and Tiros VII television picture indicating Hurricane Ginny, 1709 Z, 28 October 1963, orbit 1941.

Tropical Storm Helena

Helena developed from a slow-moving easterly wave east of the Lesser Antilles on 25 October 1963. At 1607 Z on this date, Tiros VII television cameras recorded a suspicious cloud mass near 15°N, 57°W. One of these pictures and the resulting nephanalysis are shown in Figure 41. Ships in the vicinity confirmed reports of squalls and 30 to 40 kts surface winds.

A Tiros VII radiation analysis was made over Helena at 0220 Z on 26 October which is shown in Figure 42. The storm indicated very intense high clouds (200 to 210°K) which were related to the effective radiation cloud heights respectively of 14.2 to 13.1 km level (0.1 km lower when corrected for degradation). On 26 October, Helena passed the north coast of Dominica, in the Windward Islands, where the 5000 ft mountains evidently disrupted the poorly organized storm circulation and the surface winds dropped below 30 kts.

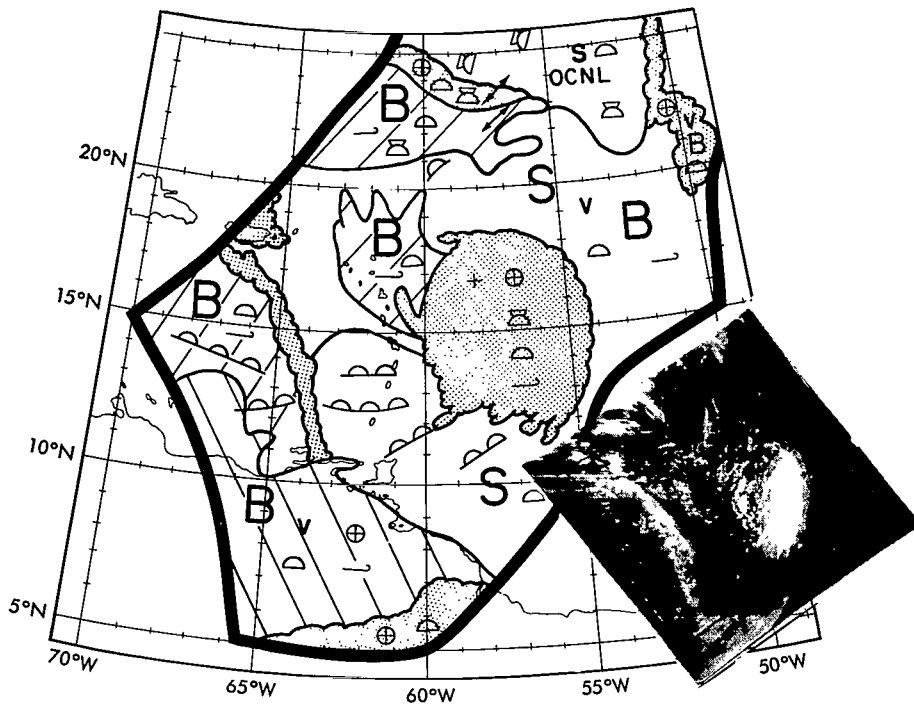


Figure 41—Nephanalysis and Tiros VII television picture indicating Tropical Storm Helena, 1607 Z, 25 October 1963, orbit 1897.

Aerial reconnaissance at 1900 Z on 27 October reported a weak wind circulation at 16° 33'N, 62° 15'W with clear skies west of 62°W. Most of the weather existed east of a line from 14°N, 65°W to 15°N, 61°W to 17°N, 60°W with cloud tops to 31,000 ft (9.4 km). Tiros VII television pictures and nephanalysis of Helena at 1508 Z on 27 October is shown in Figure 43. The storm depicted in the television pictures is confirmed in position by the 1200 Z surface chart on this date, as shown in Figure 44. The shape of the storm is strikingly similar to the Tiros VII radiation analysis at 0123 Z on 28 October, as shown in Figure 45. The high cirroform clouds (205 to 210°K) relate to the effective radiation heights respectively of the 13.8 to 13.1 km level. These cloud tops were approximately 1 km lower than those recorded on 26 October (Figure 42). It is of interest to note that Tropical Storm Helena (Figure 45) and the early formative stage of Hurricane Cindy (Figure 12) have similar cold (205 to 250°K) T_{BB} values.

Helena is an interesting example of an early stage set for favorable storm development in which a large well-developed cloud canopy existed coupled with maximum surface winds of 30 to 40 kts. But due to the interaction of external and internal dynamical and radiation forces as yet not fully understood, this warm core storm failed to become well-organized and degenerated into an area of scattered rain squalls and weak surface winds.

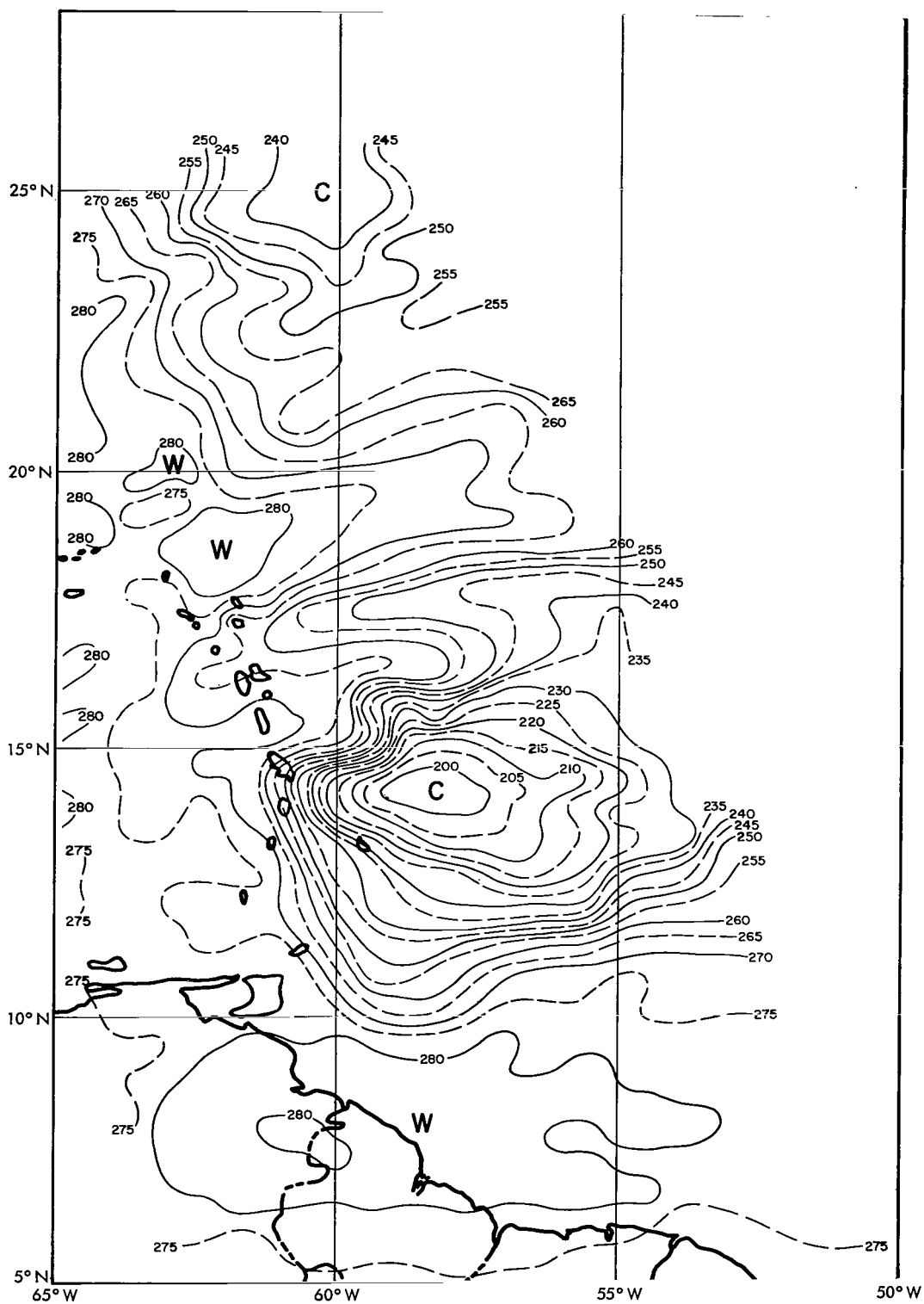


Figure 42—Channel 2 radiation analysis indicating Tropical Storm Helena, 0220–0227 Z, 26 October 1963, orbit 1903. The isolines show T_{BB} values in $^{\circ}\text{K}$ (uncorrected for instrumental degradation).

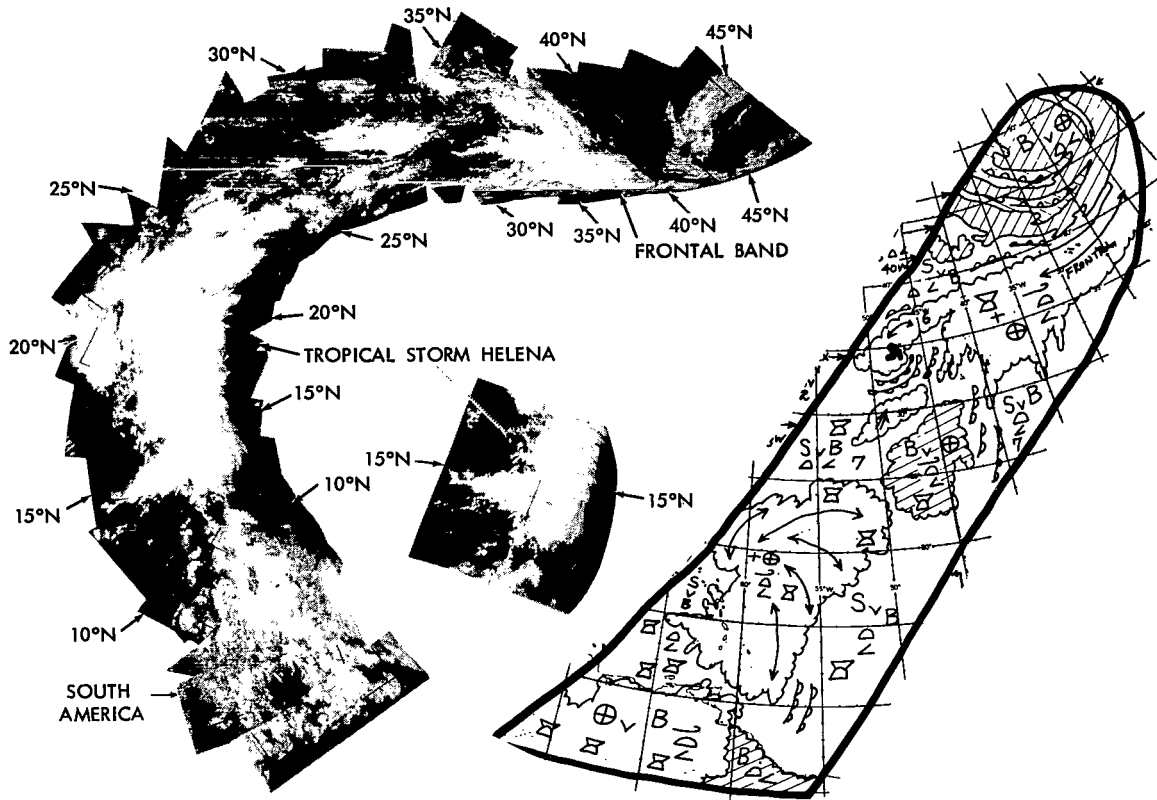
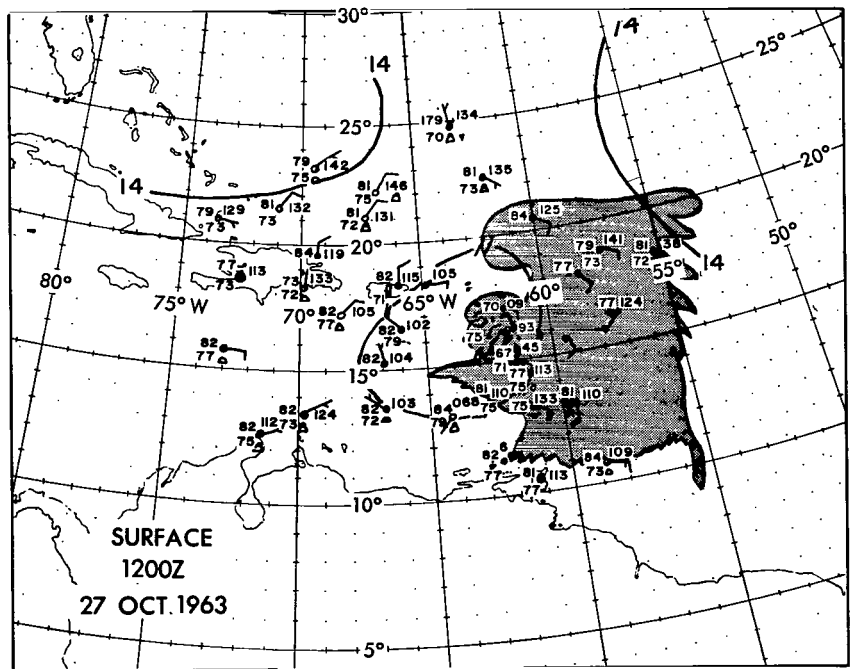


Figure 43—Mosaic and nephanalysis of Tiros VII television pictures indicating Tropical Storm Helena, 1508 Z, 27 October 1963, orbit 1925 (readout 1926).

Figure 44—Surface synoptic chart, 1200 Z, 27 October 1963, indicating Tropical Storm Helena (National Meteorological Center, U. S. Weather Bureau) with superimposed cloud nephanalysis outline.



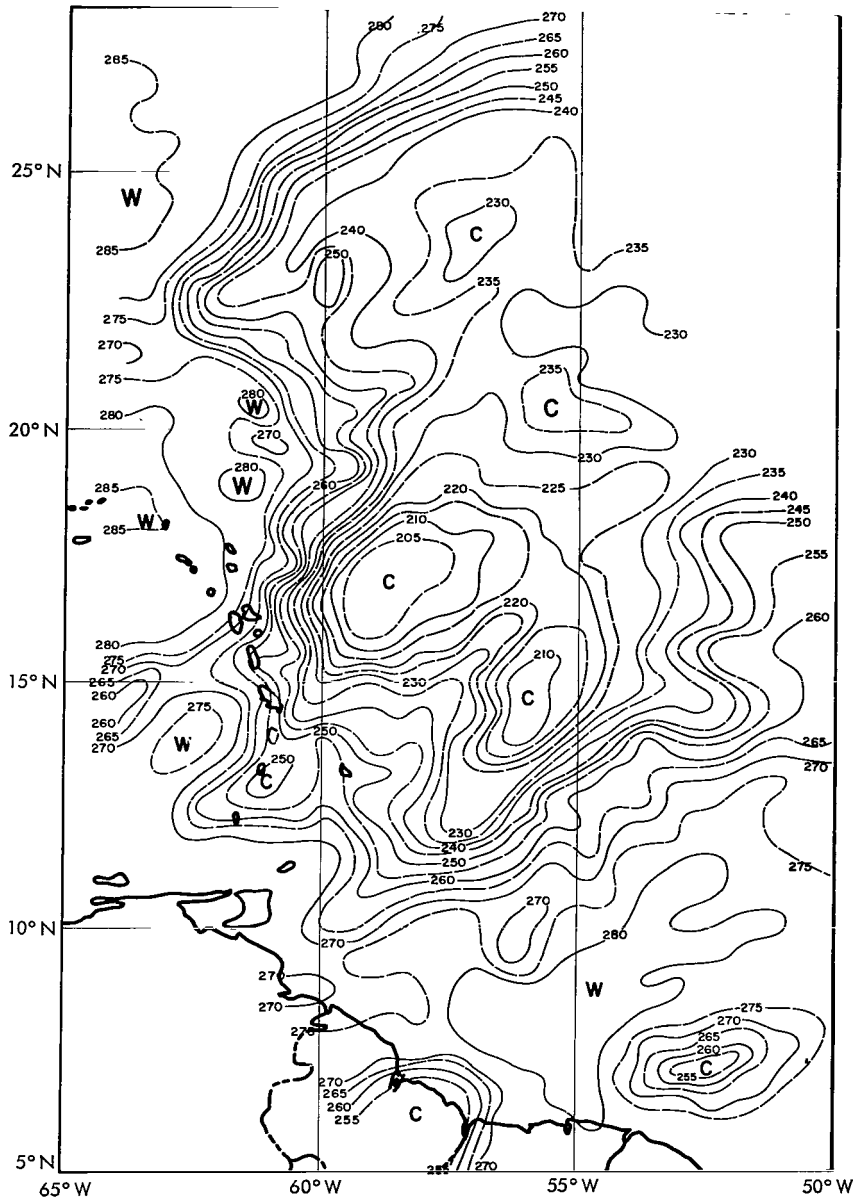


Figure 45—Channel 2 radiation analysis indicating Tropical Storm Helena, 0123-0131 Z, 28 October 1963, orbit 1932. The isolines show T_{BB} values in $^{\circ}\text{K}$ (uncorrected for instrumental degradation).

SATELLITE RADIATION DATA AND HURRICANE RESEARCH

In general, the development of a hurricane can be divided into four stages, namely, a cold core perturbation stage, a developmental transition stage, a strong, warm vortex stage and a dissipation stage (Reference 20). Observational studies have shown that many hurricanes or typhoons originate from pre-existing easterly or equatorial waves whose central cores remain relatively cold and where deepening of surface pressure seldom takes place (Reference 21). Under favorable

conditions some of the cold core high-level vortices transform into deep layer warm core vortices with the change in temperature usually taking place first at high levels (300 to 400 mb) and then spreading downward. This change is primarily due to the release of the latent heat of condensation. After this change in thermal structure takes place, the surface pressure deepens rapidly and the tangential wind intensifies (Reference 22). Riehl has noted the importance of the cirroform cloud canopy whose T_{BB} values were 200 to 210°K to the warm core formation of a hurricane (Reference 23). He estimated that a theoretical increase of upper air temperature by 1°C in 24 hours, due to the suppression of long-wave radiation could upset the balance between the warming due to the release of latent heat of condensation and the cooling due to the ascending motion of air particles. A final imbalance between the two effects could result in the final warming of the core region (Reference 24). Several schemes have been suggested to dissipate the cirroform cloud canopy above a hurricane in order to upset the radiation balance of the warm core aloft and possibly alter the 200 mb outflow pattern (Reference 25).

Riehl and Malkus have made definite observations concerning the role played by highly concentrated large diameter hot towers or giant cumulonimbus clouds which together with an oceanic heat source maintain the warm core by providing the rapid channeled ascent of warm moist surface air to high levels. The higher the released condensation heat gets before flowing out, the more effective it is in lowering the surface pressure (Reference 26). Figure 46 shows a cross-section

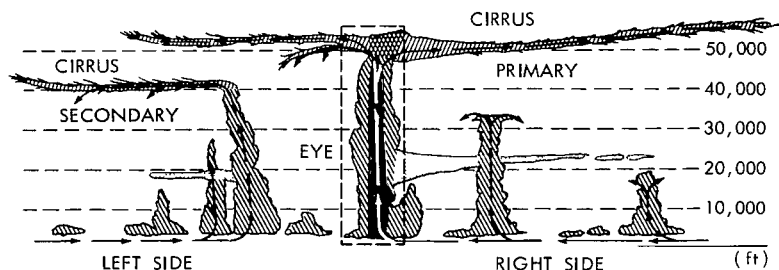
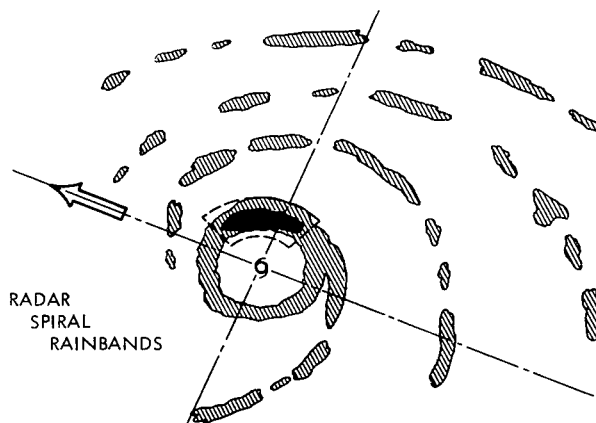


Figure 46—Hurricane model showing primary energy cells "hot towers" and secondary energy cells in the vertical and radar spiral rainbands in the horizontal (Courtesy of the U.S. Weather Bureau).



LEGEND—

- PRIMARY ENERGY CELL ("HOT TOWERS")
- ▨ CONVECTIVE CLOUDS
- ▧ ALTOSTRATUS
- ▩ CIRRUS

through a mature hurricane in which the dense hot towers occupy about 4 percent of the hurricane area. These large CB clouds become denser toward the center of the spiral rain band ring and reach a maximum concentration in the eye wall (Reference 25).

Fett has discussed the close relationship evident between the size of the cirrus cloud canopy and the intensity of the upper-level anticyclone over several typhoons in the Western Pacific (Reference 27). While Sadler has related the extent and degree of the clear area surrounding the storm to the increase in storm intensity (Reference 28). Timchalk et al. (Reference 29) have correlated the maximum surface winds to the storm's major cloud diameter and degree of "bandedness" by use of television pictures. The Tiros and Nimbus satellites with their medium and high resolution radiometer systems offer ideal platforms to detect the changes in relative size and shape of the multi-layered cloud canopies and clear areas near tropical cyclones in all stages of development. Further research work with radiation data remains to be done utilizing Timchalk's tropical cyclone classification technique in order to derive maximum surface winds and minimum surface pressure.

CONCLUSION

The role of the weather satellite as a reliable radiometric observation platform for hurricane tracking is now becoming recognized by the meteorological community. It has been shown in this study, as summarized in Table 2, that tropical cyclones from the early disturbance to the hurricane stage can have similar cold cloud T_{BB} values (205 to 220°K) and therefore minimum T_{BB} values alone are not a good measure of the stage of development of a tropical cyclone. With the initiation of further studies of satellite radiation data over additional hurricane seasons and the resulting larger statistical sample of cases, meaningful relationships should evolve between a storm's surface intensity and such radiation-derived characteristics as horizontal size, shape, and organization, in addition to the inferred cloud top heights discussed in this paper.

ACKNOWLEDGMENTS

The authors would like to thank Mr. William R. Bandeen and Capt. James S. Kennedy, U.S. Air Force, for their helpful comments and suggestions in the preparation of this study. We are particularly grateful to Major Robert W. Fett, U.S. Air Force, for his contributions and assistance in the time cross-section analysis and photo-interpretation of satellite television pictures. The nephanalyses used in this paper were provided through the courtesy of the National Weather Satellite Center, U.S. Weather Bureau, Washington, D.C.

(Manuscript received September 29, 1965)

REFERENCES

1. Bandeen, W. R., Conrath, B. J., Nordberg, W., and Thompson, H. P., "A Radiation View of Hurricane Anna from the Tiros III Meteorological Satellite," in: *Rocket and Satellite Meteorology*, ed. by H. Wexler and J. E. Caskey, Jr., Amsterdam: North-Holland Pub. Co., 1963, pp. 224-233.
2. Fritz, S., and Winston, J. S., "Synoptic Use of Radiation Measurements from Satellite Tiros II," *Month. Weather Rev.* 90(1):1-9, January 1962.
3. Allison, L. J., Gray, T. I., Jr., and Warnecke, G., "A Quasi-Global Presentation of Tiros III Radiation Data," NASA Special Publication SP-53, 1964.
4. "Annual Tropical Storm Report," Miami, Florida: U.S. Fleet Weather Facility, OPNAV Report 3140-9, March 1964.
5. Climatological Data, National Summary, Annual 1963, 13(13), Asheville, N.C.: U. S. Weather Bureau, 1964.
6. Cry, G. W., "North Atlantic Tropical Cyclones, 1964," *Mariners Weather Log*, 9(1):1-9, January 1965.
7. Dunn, G. E., et al., "The Hurricane Season of 1963," *Month. Weather Rev.* 92(3):128-138, March 1964.
8. "Surface and Upper Air Analyses," August, September, and October, 1963, National Meteorological Center.
9. Northern Hemisphere Data Tabulations - Part II, August-October, 1963, National Meteorological Center.
10. "TIROS VII Radiation Data Catalog and Users' Manual: Vol. 1, 19 June - 30 September 1963," Goddard Space Flight Center, September 30, 1964.
11. "TIROS VII Radiation Data Catalog and Users' Manual: Vol. 2, 1 October 1963 - 29 February 1964," Goddard Space Flight Center, December 31, 1964.
12. Allison, L. J. and Warnecke, G., "Examples of Certain Data Reduction and Mapping Procedures Utilizing TIROS III Five-Channel Radiometer Data," GSFC Document X-651-64-132, April 30, 1964.
13. Bandeen, W. R., "TIROS II Radiation Data Users' Manual Supplement," Goddard Space Flight Center, May 15, 1962.
14. Dunn, G. E., and Miller, B. I., "Atlantic Hurricanes," Baton Rouge, Louisiana: Louisiana State University Press, 1960.

15. Fett, R. W., "Some Characteristics of the Formative Stage of Typhoon Development: A Satellite Study," U. S. Weather Bureau, Washington, D. C., 1964.
16. Simpson, R. H., and Malkus, J. S., "Experiments in Hurricane Modification," *Sci. Amer.* 211(6):27-37, December 1964.
17. Riehl, H., Baer, F., and Vergas, K., "Prediction of Hurricane Formation in the Gulf of Mexico," Paper presented at the 3rd Technical Conference on Hurricanes and Tropical Meteorology, Mexico City, 1963.
18. Fett, R. W., "Aspects of Hurricane Structure: New Model Considerations Suggested by TIROS and Project Mercury Observations," *Month. Weather Rev.* 92(2):43-60, February 1964.
19. Fett, R. W., "Details of Hurricane Structure Revealed in Satellite Photographs," *Geofisica Internacional*, 3(4):161-164, October 1963.
20. Kuo, H. L., "On Formation and Intensification of Tropical Cyclones Through Latent Heat Release by Cumulus Convection," Chicago: University of Chicago, Department of Geophysical Sciences, Final Report, September 1964.
21. Palmer, C. E., "Tropical Meteorology," *Quart. J. Roy Met. Soc.* 78(336):126-163, April 1952.
22. Yanai, M., "A Detailed Analysis of Typhoon Formation," *Met. Soc. Jap.* 39(Set. II, No. 2):187-214, August 1961.
23. Riehl, H., "On the Origin and Possible Modifications of Hurricanes," *Science*, 141(3585):1001-1010, September 13, 1963.
24. Yanai, M., "Formation of Tropical Cyclones," *Rev. of Geophys.* 2(2):367-414, May 1964.
25. Simpson, R. H., and Malkus, J. S., "Hurricane Modifications: Progress and Prospects, 1964," Springfield, Virginia: Federal Clearinghouse for Scientific and Technical Information, NASA Contractor Report CR-59080, August 1964.
26. Riehl, H., and Malkus, J., "Some Aspects of Hurricane Daisy, 1958," *Tellus*, 13(2):181-213, May 1961.
27. Fett, R. W., "TIROS Photographs with Mosaic Sequences of Tropical Cyclones in the Western Pacific during 1962," Washington, D. C.: National Weather Satellite Center, Meteorological Satellite Laboratory, Report MSL 32, July 1964.
28. Sadler, J. C., "Satellite Meteorology Program at the University of Hawaii," Final Report of the 3rd U. S. - Asian Weather Symposium, 1st Weather Wing, Air Weather Service, 1963.
29. Timchalk, A., Hubert, L. F., and Fritz, S., "Wind Speeds from TIROS Pictures of Storms in the Tropics," Washington, D. C.: National Weather Satellite Center, Meteorological Satellite Laboratory, Report MSL 33, February 1965.

8/22/85
8

"The aeronautical and space activities of the United States shall be conducted so as to contribute . . . to the expansion of human knowledge of phenomena in the atmosphere and space. The Administration shall provide for the widest practicable and appropriate dissemination of information concerning its activities and the results thereof."

—NATIONAL AERONAUTICS AND SPACE ACT OF 1958

NASA SCIENTIFIC AND TECHNICAL PUBLICATIONS

TECHNICAL REPORTS: Scientific and technical information considered important, complete, and a lasting contribution to existing knowledge.

TECHNICAL NOTES: Information less broad in scope but nevertheless of importance as a contribution to existing knowledge.

TECHNICAL MEMORANDUMS: Information receiving limited distribution because of preliminary data, security classification, or other reasons.

CONTRACTOR REPORTS: Technical information generated in connection with a NASA contract or grant and released under NASA auspices.

TECHNICAL TRANSLATIONS: Information published in a foreign language considered to merit NASA distribution in English.

TECHNICAL REPRINTS: Information derived from NASA activities and initially published in the form of journal articles.

SPECIAL PUBLICATIONS: Information derived from or of value to NASA activities but not necessarily reporting the results of individual NASA-programmed scientific efforts. Publications include conference proceedings, monographs, data compilations, handbooks, sourcebooks, and special bibliographies.

Details on the availability of these publications may be obtained from:

SCIENTIFIC AND TECHNICAL INFORMATION DIVISION
NATIONAL AERONAUTICS AND SPACE ADMINISTRATION

Washington, D.C. 20546